
Distribution of the organic matter in the channel-levees systems of the Congo mud-rich deep-sea fan (West Africa). Implication for deep offshore petroleum source rocks and global carbon cycle

François Baudin^{a,*}, Jean-Robert Disnar^b, Philippe Martinez^c and Bernard Dennielou^d

^a UPMC – Univ. Paris 06/CNRS, UMR 7193 ISTeP, Equipe Evolution et Modélisation des Bassins Sédimentaires, case 117, 4 place Jussieu, 75252 Paris Cedex 05, France

^b Université d'Orléans/CNRS/Université François Rabelais-Tours, UMR 6113 Institut des Sciences de la Terre d'Orléans, Campus Géosciences, 1A rue de la Férollerie, 45071 Orléans Cedex 2, France

^c Université Bordeaux 1/CNRS, UMR 5805 EPOC, avenue des facultés, 33405 Talence Cedex, France

^d Ifremer, Département des Géosciences Marines, BP 70, 29280 Plouzané Cedex, France

*: Corresponding author : François Baudin, email address : francois.baudin@upmc.fr

Abstract:

The quantity and the source of organic matter preserved in the Recent turbiditic channel-levees systems around 4000 m-depth off the Congo River were determined using bulk geochemical approaches (Rock-Eval, elemental and isotopic analyses) as well as molecular and optical analyses on selected samples. These mud-rich sediments contain high amount of organic matter (3% Corg on average), the origin of which is a mixture of terrestrial higher-plant debris and deeply oxidized phytoplanktonic material. Although the relative contribution of continental source versus marine source of the organic matter cannot be precisely quantified, the continental fraction appears significant (at least 70–80%) especially for such depths and distances from the coast. The organic matter distribution appears very homogeneous at different scales, from the single turbiditic event to the entire levee, and changes in accumulation rates have a little impact on the quantity and quality of preserved organic matter.

With a petroleum potential around 4.5 kg HC per t rock, the fine-grained turbiditic sediments in the Congo deep-sea system could be regarded as an analog of gas-prone source rocks for the deep offshore of the Atlantic margins. Finally, the Congo deep-sea turbiditic system is a major conveyor of organic carbon to the deep ocean. Further studies are needed to evaluate the efficiency of such systems for the storage of continental organic matter into the deep ocean in relation to sea-level and climatic changes.

Keywords: South-East Atlantic; Turbidites; Carbon isotopes; Nitrogen isotopes; Biomarkers; Source rocks

1. Introduction

With deep-water exploration for petroleum purposes becoming more intensive and successful, it is clearly important to have a better knowledge of the depositional processes of source rocks, reservoirs and seals in the deep sea. Up to now, deep-water reservoirs have received most of the attention from the scientific community whereas the source rocks have been less studied. According to conventional views, deep water settings are not suitable for source rock deposition because organic material is intensely degraded during settling through the water column. However several transport processes exist that may lead to deposition of organic-rich sediments in the deep sea, which can now be regarded as areas favourable for the occurrence of potential hydrocarbon source rocks (Huc et al., 2001; Stow et al., 2001; Saller et al., 2006). Sediment mass transport processes such as turbidity currents provide one efficient way for accumulating both terrestrial and marine organic-rich fine-grained sediments in the deep offshore.

Clay rich fine-grained turbidites are particularly well developed as levees in the deep-sea turbidite systems and are therefore also closely associated to sandy reservoirs that are turbiditic channels. These shaly facies usually act as seals in the petroleum system, but their potential as source rock is poorly known. Moreover, these facies are widely distributed from the upper slope to the distal part of the deep sea turbidite systems, in the abyssal plains, and represent huge volume of sediment in which organic matter can be preserved. The contribution of such facies to the global carbon budget is still poorly constrained.

We attempt here to quantify the organic matter preserved in the channel-levees systems from the Congo mud-rich deep-sea turbidite system as well as to determine its origin (terrestrial versus marine) in order to discuss the importance of such facies in terms of potential petroleum source rocks and their contribution for carbon storage.

2. General setting and studied sites

2.1 General setting

The Zaire/Congo River drains the second largest catchment area of the world ($3.7 \cdot 10^6$ km², Fig. 1) and about 38% ($42,800 \text{ m}^3/\text{s}$ or $1350 \text{ km}^3/\text{year}$) of the yearly run-off from Africa

76 occurs through this river (Kinga-Mouzeo, 1986; N’Koukou and Probst, 1987). Although the
77 Congo River shows a small variability in its flow (22,000 to 76,500 m³/s), floods are recorded
78 in May and December.

79 The Congo River delivers yearly ~55 10⁶ t of suspended sediment (Wetzel, 1993), that
80 is 15 to 17 times lower than the Amazon River which has a drainage basin only 2 times higher
81 and a fluid discharge of 130,000 m³/s. This difference is attributed to the flat morphology of
82 the catchment area of the Congo River and to the presence of several lakes through its course
83 that trap an important part of the suspended material (N’Koukou and Probst, 1987).

84 Despite its relatively low sedimentary load, the Congo River contributes to 3.9% (13 10⁶ t
85 C/year) of the global annual supply of terrigenous organic carbon into the ocean (Martins and
86 Probst, 1991). The dissolved organic carbon and particulate organic carbon near the mouth
87 are 8.5 and 1.0 mg/L, respectively (Meybeck and Ragu, 1996; Coynel et al., 2005).
88 Consequently, the particulate organic carbon/suspended material ratio delivered by the Congo
89 River is high (1/20) compared to other major rivers with higher sedimentary loads, e.g. 1/50
90 for the Amazon River.

91 The freshwater outflow of the Congo River into the Atlantic Ocean is detectable by
92 reduced salinity in a 5-10 m thick surface layer as far as 800 km offshore (van Bennekom and
93 Berger, 1984). This freshwater outflow, rich in phosphate and nitrate, induces upwelling and
94 two nearshore coastal cells are seasonally observed just south and north of the Congo mouth
95 at 5 and 7° S (Fig. 1). They are considered to be produced by the piling up of eastward-
96 flowing equatorial undercurrents as they arrive at the continental margin off Congo and
97 Gabon (Voituriez and Herbland, 1981; Servain et al., 1982). As a result of oceanic or river-
98 induced upwellings and the supply of nutrients by the Congo River, the primary productivity
99 is high in the surface waters in that part of the Atlantic Ocean. Berger (1989) gives values of
100 90-125 g C/m²/year for the area off the Congo mouth and slightly higher values, between 125
101 and 180 g C/m²/year, for the oceanic upwelling area off Angola.

102 The strong influence of the river sediment load on the adjacent continental margin is
103 evident from the existence of the Congo mud-rich deep sea turbidite system. This edifice is
104 one of the world’s largest active deep sea turbidite systems, with an area estimated to 330,000
105 km² (Savoye et al., 2000). Owing to the narrow (~50 km wide) continental shelf in front of
106 the Congo mouth and the presence of a canyon that begins 30 km within the estuary of the

107 river (Fig. 1 and Fig. 2), a large part of the sediment load, including organic matter, is
108 transported directly into the deep-sea.

109 The modern active canyon/channel system extends 760 km westward off the Congo-Angola
110 margin (Fig. 2), but more than 80 inactive paleo-channels have been identified (Savoye et al.,
111 2000; Savoye et al., 2009). The canyon/channel deeply incises the continental shelf and slope,
112 and is very meandering (Droz et al., 1996; Savoye et al., 2000; Fig. 2). The sinuosity of the
113 modern channel decreases downslope from high to moderate (Babonneau et al., 2002). A
114 transition zone starts at about 3300 m-depth and links the canyon area to the channel-levees
115 system (Babonneau et al., 2002). The channel-levees system shows an east-west trend, but
116 abrupt changes of the direction are observed locally (Savoye et al., 2000). The slope of the
117 channel floor decreases from 1.5 to 0.2% down channel. The channel is over-incised, with an
118 incision depth ranging from 200 m at 3000 m-depth to 100 m at 4300 m-depth (Savoye et al.,
119 2000).

120 Evidence for the occurrence of turbidity currents in the canyon/channel includes
121 submarine cable breaks between 500 and 2300 m-depth, which were attributed to turbidity
122 currents initiated by Congo floods (Heezen et al., 1964). During long-term monitoring along
123 the channel using a series of moorings with currentmeters and sediment traps, several
124 turbiditic events were recorded between 2001 and 2004 (Khripounoff et al., 2003;
125 Vangriesheim et al., 2009). The frequency of turbiditic events is estimated of ca. 60 per
126 century (Heezen et al., 1964), but it is not clear where those turbidity currents start and what
127 causes them.

128 Turbidity currents are supposed to remain within the canyon/channel all the way down, but in
129 the meander section the upper part of the thick turbidity currents overflows the channel flanks
130 and built levees. Levees are evidenced by seismic surveys all along the present-day active
131 channel. Levees are made up of overflow sedimentation of the turbidity currents on both sides
132 of the channel with a relatively symmetrical morphology; the Coriolis force being negligible
133 in this area given the proximity to the Equator. The lateral extent of levees decreases from 50
134 to 10 km down slope (Savoye et al., 2000). The presence of sediment waves has also been
135 reported on both right-hand and left-hand levees (Droz et al. 1996; Savoye et al., 2000;
136 Migeon et al., 2004). The frequency of overbank depositional events at the lower channel-
137 levees system is estimated at 2 per century (Savoye et al., 2009).

138 To the best of our knowledge, information about the nature of organic matter from the
139 channel-levees systems is lacking. The main objective of the present paper was to provide
140 insight into the nature and distribution of the organic matter at different scales in the modern
141 channel-levees system.

142 143 **2.2 Studied areas**

144 Two areas were selected along the modern active channel in the lower part of the
145 channel-levees system (Fig. 2). Both are composed of three cores that allow study of a
146 transect from the channel to the external part of the levees.

147 148 *Transect KZAI 04-06 (Figs. 2 and 3)*

149 This transect is located at 712 km from the apex of the canyon, following the main
150 active channel, and is between 4000 and 4150 m-depth. The cores are located in an area
151 where the channel is relatively straight, with a width around 1.6 km and a depth nearly 150 m
152 (Gervais et al., 2001; Fig. 2). Lateral extension of the south levee, studied here, is around 7
153 km. Levees are symmetrical and show sediment waves with NW–SE orientation, i.e.
154 approximately at 45° of the channel direction (Fig. 2; Gervais et al. 2001). One core (KZAI
155 06) has been collected in the channel at 4150 m-depth, one core (KZAI-05) has been collected
156 on the proximal part of the levee at 4012 m-depth and one core (KZAI-04) has been collected
157 on the distal part of the levee at 4047 m-depth (Fig. 3). A seismic profile (Fig. 3) shows that
158 core KZAI 05 is close to the crest of the south levee and that core KZAI 04 is 5 km apart
159 where seismic facies are more continuous and bedded. It should be noted that 10 km upstream
160 of the studied area the Congo channel forms a well-developed meander (Fig. 2) that may be a
161 subordinate source of sediments in core KZAI 05, as suggested by the orientation of the field
162 of sediment waves connected to this meander.

163 Gervais et al. (2001) indicate that sediments from cores KZAI 04 (16.9 m long) and
164 KZAI 05 (13.3 m long) are made of clayey and silty clayey sequences showing millimetric
165 silt beds layered with millimetric to decimetric clay beds (Fig. 3). These small sequences are
166 fining-up and correspond to Td and Te terms of the Bouma sequence or the fine-grained
167 turbidites defined by Piper (1978). Turbiditic clay cannot easily be distinguished from
168 hemipelagic clay. Most of the components of the sediment (quartz, micas, plant fragments,
169 benthic foraminifers) have an allochthonous origin, whereas some diatoms and sponge

170 spicules constitutes a minor autochthonous component of the sediment. Both cores show the
171 same type of sequences, although core KZAI 04 (more distant from the channel compared to
172 core KZAI 05) shows a lower proportion of fine to medium sand fraction. This maybe reflects
173 the lower sediment accumulation rate, which is averaged to 0.79 m/ka for core KZAI 05 to
174 0.44 m/ka for KZAI 04 (Gervais et al., 2001).

175 Sediments from core KZAI 06 (3.3 m long) are made of medium (250-500 μm) to fine (250-
176 125 μm) homogeneous sands, containing some mud clasts and large plant debris. The 20 cm
177 at the top of this core includes silty clays with some sandy lenses (Gervais et al., 2001).

178

179 *Transect KZAI 13-15*

180 This transect is located at 855 km from the apex of the canyon at about 4350 to 4450
181 m-depth (Fig. 2). The studied levees are located on the left-hand flank of a meander (1 km of
182 curvature) and show marked sediment waves. The relief is 90 m between the channel and the
183 crest of the levee. Crests of proximal sediment wave mimic the curvature of the meander, and
184 then become straighter down-levee (Fig. 2).

185 Core KZAI 15 (1.9 m long) was collected in the channel and consists of very fine (100 μm) to
186 very coarse (1–2 mm) sand beds with abundant scattered mud clasts (Fig. 3). Accumulation
187 rates are very low, 0.25 m/ka according to Migeon et al. (2004), confirming that the channel is
188 a zone of sediment bypassing and/or erosion rather than deposition.

189 Cores KZAI 13 (17.9 m long) and KZAI 14 (17.3 m long) were collected respectively on the
190 downstream and upstream flank of a sediment wave (Fig. 2). Core KZAI 13 is 0.2 km
191 downstream from core KZAI 14, the latter being located at 1 km from the axis of the channel.

192 Both are made of clayey and silty clayey sequences showing millimetric silt beds
193 layered with millimetric to decimetric clay beds (Fig. 3). Accumulation rate is difficult to
194 estimate because some inversions of the ^{14}C ages are observed in both cores (Migeon et al.,
195 2004). Nevertheless, the average accumulation rate seems fluctuate from 6.5 m/ka in core
196 KZAI 13 and 4.4 m/ka in core KZAI 14. Such values suggest that the mean accumulation rate
197 of levees sharply increases from the area of transect KZAI 04-06 to this area, although the
198 lithology of sediments does not change a lot (Denniellou and Jouanneau, in press; Savoye et
199 al., 2009).

200

201 **3. Material and methods**

202
203
204
205
206
207
208
209
210
211
212
213
214
215
216
217
218
219
220
221
222
223
224
225
226
227
228
229
230
231
232
233
234
235
236
237
238
239
240
241
242
243
244
245
246
247
248
249
250
251
252
253
254
255
256
257
258
259
260
261
262
263
264
265

202

1 203 **3.1 Samples**

3 204 Three hundred and sixteen (316) samples were collected from these six cores with
4 spacing between samples varying from 2 to 20 cm (Tab. 1). Only the first 10 m of cores KZAI
5 205 04, 05, 13 and 14 were sampled (Fig. 3).
6

7 206
8
9 207 In the laboratory, the samples were washed with deionized water to eliminate salt
10 that could affect pyrolysis analyses. Indeed, salt generates an artefact at the end of the S₂ peak
11 208 of the Rock-Eval pyrolysis (see below), which is erroneously interpreted as a fraction of
12 209 refractory organic matter coming from soils (Holtvoeth et al., 2005). Then, samples were
13 210 dried in an oven at 50 °C for 24 hours before being pulverized in an agate mortar.
14
15
16 211
17

18 212 19 20 213 **3.2 Methods**

21 214 Grain-size of the bulk sediment was measured using a Coulter LS200 (93 channels
22 from 0.4 µm to 2 mm).
23
24

25 216 Carbonate content was measured using a Bernard calcimeter, with an analytical
26 precision of ± 0.2% CaCO₃.
27 217

28
29 218 Pyrolytic analyses were carried out using both an Oil Show Analyser and a Rock-Eval
30 6 Turbo device (Vinci Technologies), operating in free cycle mode which is devoted to
31 219 Recent sediments (Espitalié et al., 1985; Lafargue et al., 1998; Béhar et al., 2001). This
32 220 technique provides five fundamental parameters: S₁ (representing free and adsorbed
33 221 hydrocarbons released during 3 min at 180 °C, in mg/g); S₂ (pyrolytic hydrocarbons generated
34 222 from 180 to 650 °C, in mg/g); S₃ (CO₂ released during the pyrolysis phase of the analysis, in
35 223 mg CO₂/g); S₄ (CO₂ released during the oxidation phase of the analysis, in mg CO₂/g); and
36 224 Tmax (the temperature of maximum pyrolytic hydrocarbon yield, in °C). Hydrocarbons are
37 225 detected by a flame ionization detector, and CO₂ by a thermal conductivity detector or infra-
38 226 red detector.
39
40
41
42
43
44
45
46

47 228 These fundamental parameters are used to obtain derived parameters that are: TOC (Total
48 229 Organic Carbon, in wt %); Hydrogen Index (HI = S₂/TOC × 100, in mg HC/g TOC); Oxygen
49 230 Index (OI = S₃/TOC × 100, in mg CO₂/g TOC); and Petroleum Potential (PP = S₁+S₂, in mg
50 231 HC/g or kg HC/ton of rock). The precision for the parameters is ± 0.1% for TOC, ± 1 °C for
51 232 Tmax, ± 10 mg HC/g TOC for HI, ± 5 mg CO₂/g TOC for OI, and ± 1 kg/t for PP.
52
53
54
55
56
57
58
59
60
61
62
63
64
65

233 C/N and isotopic ratios were determined on 50 selected samples from cores KZAI 04,
234 05 and 13. Samples were acidified with 1N HCl to remove inorganic carbon prior to carbon
235 isotopic measurements. Total Organic Carbon (TOC) and Total Nitrogen (TN) were measured
236 by high temperature combustion on a Carlo Erba NC 2500. The average standard deviation of
237 each measurement, determined by replicate of the same sample is $\pm 5\%$

238 Stable carbon and nitrogen isotope composition of the sedimentary organic matter was
239 determined by on-line combustion in a Carlo Erba NC 2500 interfaced with a Isoprime
240 isotope ratio mass-spectrometer. $^{13}\text{C}/^{12}\text{C}$ and $^{15}\text{N}/^{14}\text{N}$ are expressed by the conventional δ
241 notation in ‰ relative to PDB and air, respectively. Analytical precision is ± 0.15 ‰ for
242 $\delta^{13}\text{C}_{\text{org}}$ and ± 0.2 ‰ for $\delta^{15}\text{N}$.

243 Thermochemolysis was carried out on 9 samples from cores KZAI 04, 05, 13 and 15
244 following the procedure described by Disnar et al. (2008). Briefly, about 25 mg of dried and
245 crushed kerogens were introduced in SVL® screw-cap glass tubes with 50 μL of standard
246 solution (heptylbenzoic acid 21 $\mu\text{g}/100$ μL MeOH) and 100 μL tetramethyl ammonium
247 hydroxide solution (TMAH; 25 % in MeOH). The tubes were placed open in an oven at 75 °C
248 for 3 to 5 hours to evaporate the excess methanol, then cooled and closed under vacuum. Then
249 they were placed vertically in a sand-bath and heated at 220 °C during 20 min. After cooling
250 in ambient air, 1.5 mL diethylether was introduced to extract the pyrolysis products. After
251 evaporation of the ether, the extracts were diluted in 50 or 100 μL CH_2Cl_2 and analysed by
252 GC-MS with a Thermo-Finnigan TRACE-Polaris GCQ gas chromatograph–mass
253 spectrometer. The gas chromatograph was fitted with an Rtx™-5Sil MS capillary column (30
254 m x 0.32 mm i.d., 0.25 μm film thickness) with 5 m of guard column. The GC operating
255 conditions were as follows: temperature hold at 40 °C for 1 min, then increase from 40 to 120
256 °C at 30 °C/min, 120 to 300 °C at 3 °C/min with final isothermal hold at 300 °C for 30 min.
257 The samples were injected splitless, with the injector temperature set at 280 °C. Helium was
258 the carrier gas. The mass spectrometer was operated in the electron ionization (EI) mode at 70
259 eV ionization energy and scanned from 50 to 650 Daltons. Compounds were tentatively
260 identified by comparison with library (NIST) mass spectra and relative retention times.

261 Forty-five samples were selected and prepared for palynofacies analysis, which is the
262 microscopical study of all the particulate organic matter present in sediment. Neither
263 oxidation nor ultrasonic probe was carried out during processing as all the particles were of

264 interest in this study and may selectively be destroyed by such procedures. The residue was
265 directly mounted on glass microscope slides.

266 The classification of palynofacies has always been rather subjective (Tyson, 1995),
267 and for this study, the following particles were identified:

- 268 – Phytoclasts: comprise all opaque and translucent land-plant debris. Different
269 subgroups can be observed within this fraction and they were distinguished during
270 the counting.
- 271 – Sporomorphs: comprise the land-derived pollen grains and spores.
- 272 – Fungal debris: comprise all the filamentous segmented particles and sclerotes.
- 273 – Marine algae: comprise the dinoflagellate cysts and other organic walled algae.
- 274 – Amorphous organic matter (AOM): comprise all particulate organic components
275 that appear structureless at the scale of light microscopy.

277 4. Results

278 4.1 Organic matter distribution and characteristics in the clayey-silty facies of the levees

279 Grain-size determinations indicate that most of the sediment is made by clayey and
280 silty fractions (up to 80 to 90%) with a median grain-size around 10 μm for cores KZAI 04
281 and 05 and 15 μm for cores KZAI 13 and 14 which are located at 1 km from the axis of the
282 channel (Fig. 4). The sandy fraction usually represents less than 15% in cores KZAI 04 and
283 05 and less than 20 % in cores KZAI 13 and 14, except for various short-term spikes (30% in
284 cores KZAI 04 and 05, 40 % in core KZAI 14 and up to 50% in core KZAI 13) which
285 correspond to coarser turbiditic events.

286 Calcium carbonate contents remain generally low (<6 %, Tab. 2) with an average
287 around 2.5 %. Thus, these sediments can be regarded as virtually devoid of carbonate.

288 Total Organic Carbon (TOC) contents are extremely homogeneous in the four studied
289 cores with a value around 3% (Tab. 2). Some samples, however, are richer in organic carbon
290 with a TOC content reaching 5.6% in core KZAI 04, whereas others show values as low as
291 0.1 % in core KZAI 13 (Fig. 4). These organic-lean samples correspond to the sandy turbiditic
292 facies. Except for these rare sandy facies, no relationship appears between TOC and the
293 granulometric characteristics of the sediment.

295 Hydrogen Index (HI) values fluctuate between 82 and 236 mg HC/g TOC (Tab. 2)
1 296 with a mean value around 145 mg HC/g TOC in the four studied cores (Fig. 4). The HI-values
2 297 are extremely constant in cores KZAI 04 and 05 and show a wider range and more abrupt
3 298 fluctuations in cores KZAI 13 and 14 (Fig. 4). Nevertheless, these variations are not very
4 299 important if we consider that HI-values may fluctuate from 0 to 1000 (Espitalié et al., 1985).

8
9 300 C/N ratios are also very homogeneous with a mean C/N ratio around 13 (range
10 301 between 10.7 and 15.7). Similarly, isotopic ratios do not vary greatly with a mean $\delta^{13}\text{C}_{\text{org}}$
11 302 around -26 ‰ (range between -23.8 and -27.1 ‰) and a mean $\delta^{15}\text{N}$ around 5.5 ‰ (range
12 303 between 5 and 6.3 ‰; Tab. 2 and Fig. 4).

16 304 Palynofacies analyses indicate that amorphous organic matter (AOM) represents
17 305 almost the half of total particles (between 33 and 62% with an average around 46.5%). The
18 306 AOM particles can be classified into two main subgroups. The first subgroup is composed of
19 307 fluffy AOM (Fig. 5A) which is probably derived from phytoplankton. The second subgroup is
20 308 represented by AOM particles with remains of phytoclasts inside (Fig. 5B). Variations in
21 309 AOM aspect probably highlight the origin of the organic matter (marine versus terrestrial) but
22 310 also the role of the depositional setting, i.e. the intensity of oxidation.

27 311 The structured particles consist exclusively of higher plant debris at different states of
28 312 preservation. Different types can be recognized from yellow coloured cuticles or woody fibres
29 313 with well preserved cellular structures (Fig. 5C) to dark-brown and gelified ligno-cellulosic
30 314 debris (Fig. 5D). Ligno-cellulosic particles represent between 20 and 53% (34% on average)
31 315 of total particles. Black particles with different shapes, rounded or bladed, are a subordinate
32 316 group of phytoclasts and represent char or highly oxidized particles from soil (Fig. 5E).
33 317 Cuticles are present at a low level (0.5 to 6%), whereas sporomorphs are rare (< 2% on
34 318 average; Fig. 5F). Fungal remains are frequent and may represent few percents in some
35 319 samples. Marine palynomorphs are scarce in the palynofacies. To summarize, the palynofacies
36 320 analysis indicates that half of the organic matter is clearly terrestrial in origin, and part of the
37 321 amorphous organic matter is also derived from higher plants.

49 322 At the scale of the bulk sediment of the levees the organic matter content appears very
50 323 homogeneous, both in terms of quantity (TOC) and quality (HI, C/N and isotopic ratios,
51 324 palynofacies).

56 326 **4.2 Organic matter distribution and characteristics in the turbiditic beds**

327 Using detailed lithological descriptions, X-radiographs, and grain size analyses, six
1 328 types of turbiditic beds have been distinguished within the levees (Gervais et al., 2001;
2 329 Migeon et al., 2004). We sampled several of these beds with a 2 cm-spacing in cores KZAI
3 330 04, 13 and 14 in order to investigate the variations of organic matter content and its quality
4 331 within different types of small fining-up sequences.
5 332

6 333 Type 1-beds consist of highly bioturbated dark silty clays grading upward into grey
7 334 clays, with thickness ranging from several centimeters to several decimeters (Fig. 6A and B).
8 335 Dark silty clays are probably true turbidite deposits whereas grey clays are probably
9 336 hemipelagic deposits, but discriminating between them is difficult (Migeon et al., 2004). In
10 337 most cases, the grain size is near constant whatever the facies. The organic matter content of
11 338 both the dark and grey clays is very homogeneous (3% in average), but dark clays may
12 339 contain a little bit more organic matter than grey hemipelagic clays (Fig. 6B). Such beds
13 340 resulted from fallout of suspended flocks and characterize dilute and low-velocity spillovers
14 341 from the uppermost part of channelized turbidity currents (Migeon et al., 2004).
15 342

16 343 Type 2-beds show a basal unit with the alternation of infra-millimetric to millimetric
17 344 silty laminae and millimetric to centimetric clayey laminae, and an upper unit with dark silty
18 345 clays grading upward into grey clays (Fig. 6C and D). The basal contact is always sharp and
19 346 beds present thickness ranging from 5 to 30 cm. The contact between the two units is
20 347 gradational, the whole sequence is normally graded, and grain-size analyses display several
21 348 normally graded sub-intervals. Bioturbation is always absent from the basal unit but
22 349 commonly observed in the upper unit. The absence of bioturbation in the basal unit suggests
23 350 rapid deposition by a single channelized turbidity current. Such type 2-beds result from the
24 351 spillover of the upper muddy part and deeper parts of channelized flows, where silts are
25 352 carried in suspension, and correspond to divisions Td and Te of the Bouma sequence (Gervais
26 353 et al. 2001; Migeon et al., 2004). The organic matter content of such type 2-beds are usually
27 354 high (3% TOC) except in the first coarser centimeters of the basal unit where lower TOC
28 355 content are noted (1.5 to 2%; Fig. 6D).
29 356

30 357 Type 3-beds consist of three units: from base to top, dark silty clays 1–3 cm thick (unit
31 358 1), alternating silty and clayey laminae (unit 2), and grey clays (unit 3; Fig. 6E). All contacts
32 359 between the three units are gradational. In unit 2, silty laminae first coarsen and thicken
33 360 upward, then fine and thin upward. The whole bed exhibits a basal inverse grading and an
34 361 upper normal grading. The basal contact is sharp or gradational. Bed-type 3 is uncommon and
35 362
36 363
37 364
38 365
39
40
41
42
43
44
45
46
47
48
49
50
51
52
53
54
55
56
57
58
59
60
61
62
63
64
65

359 its thickness varies between 10 and 20 cm (Migeon et al., 2004). Organic carbon content of
1 360 such beds shows a wider range in accordance with the median grain size. As coarser the
2 361 sediment as lower the organic matter content, with values as low as 0.2% in fine sands (Fig.
3 362 6E).

7 363 Type 4-beds consist of three units from base to top: a centimeter-scale silty bed
8 364 passing upward to alternating silty and clayey laminae, and finally grey to beige clays (Fig.
9 365 6F). The basal silty bed is structureless, and rarely laminated or cross-laminated. The whole
10 366 bed is normally graded, and the basal contact is sharp. This type 4-bed has thickness varying
11 367 between 10 and 30 cm and result from processes similar to those described for deposition of
12 368 type 2-beds (Migeon et al., 2004). Organic carbon content is almost constant (3 % TOC)
13 369 within this type 4-beds except at the basal part of the small sequence when grain size
14 370 increases (Fig. 6F).

21 371 Types 5 and 6-beds are rare, different from the classical fine-grained deposits
22 372 commonly described on levees as they correspond to structureless Ta and/or laminated Tb of
23 373 the Bouma sequence with maximum grain-size up to 400 μm (Migeon et al, 2004). They were
24 374 not studied so far for their organic matter content.

29 375 Whatever the small changes in organic matter content within the small-scale fining-up
30 376 sequences described above, they are not associated with lower HI-values. On the contrary,
31 377 both HI and OI-values are rather constant (Fig. 6), which indicates a similar type of organic
32 378 matter and probably a comparable preservational state of the organic particles in these
33 379 different facies.

40 381 **4.3 Organic matter in the sandy facies of the channel**

42 382 The sandy facies from the channel have been analyzed in core KZAI 15 and only 4
43 383 samples were investigated. Even if we cannot generalize these observations, it appears that the
44 384 sands contain two times less organic carbon than the clayey facies (Tab. 2). The HI-values of
45 385 the sandy facies from the channel are quite comparable with that of levee facies (Tab. 2) and
46 386 geochemical data indicate the same molecular proportion of terrestrial organic material and
47 387 the same state of degradation compounds from lignin (see TMAH results in section 5.1 and
48 388 Tab. 4). It suggests that size sorting, which explain the difference in TOC between channel
49 389 and levee, did not influence the quality of particulate organic sediment. Any generalization of
50
51
52
53
54
55
56
57
58
59
60
61
62
63
64
65

390 these observations for the entire Congo deep-sea turbiditic system is limited because of the
391 small number of the samples in our study.

393 5. Discussion

395 5.1 Sources of organic matter and estimation of the terrestrial organic carbon 396 contribution

397 The identification and quantification of sources, whether terrestrial or marine, of
398 organic carbon in the sediment are always difficult because several parameters influence the
399 bulk and molecular characteristics of the preserved organic matter. In order to estimate the
400 amount of terrestrial organic matter relative to total organic matter in the Congo deep sea fan
401 sediments we used binary mixing models with different sets of proxies (HI, C/N ratio,
402 $\delta^{13}\text{C}_{\text{org}}$ and $\delta^{15}\text{N}$), defined as follow:

$$403 \quad F_{\text{ter}} = [(X_{\text{sample}} - X_{\text{mar}}) / (X_{\text{ter}} - X_{\text{mar}})] \times 100$$

404 Where F_{ter} is the terrestrial organic carbon fraction and X_{sample} is depending on the proxy
405 analysed. X_{mar} and X_{ter} are the marine and terrestrial end-member values, respectively, of
406 these proxies.

408 Information on the origin of organic matter can be achieved by pyrolytic
409 measurements if the thermal evolution of organic matter is low (Espitalié et al., 1985; Peters
410 et al., 1986). Measured T_{max} values are always low ($< 420^\circ\text{C}$), indicating that organic matter
411 did not experience strong thermal maturation and therefore contains very little charcoals or
412 recycled material from older mature rocks.

413 Although the type of organic matter is usually defined by the mean of elemental
414 analysis, the Hydrogen Index (HI) parameter approximates the H/C atomic ratio, which
415 determines the organic matter type (Tissot and Welte, 1984). According to the low range of
416 HI values (82 to 236 mg HC/g TOC, Tab. 2), the organic matter of the studied samples could
417 be attributed mainly to Types III to IV (Fig. 7). Type IV, however, appears as a subordinate
418 type for some samples (Fig. 7). Type III is usually related to terrestrial higher plants debris,
419 whereas Type IV corresponds to residual deeply altered organic matter; the origin of which is
420 difficult to determine.

421 If we assume that HI value for fresh marine organic matter is around 400 mg HC/g
422 TOC (Espitalié et al., 1985) and around 100 for the terrigenous end-member (mixture of
423 Types III-IV; Espitalié et al., 1985), the mean F_{ter} value calculated in the studied cores would
424 indicate that 85% of the organic matter is derived from the detrital source (Tab. 3). Taking
425 into consideration the highest HI values measured on every core (Tab. 2), the terrestrial
426 contribution drops to 67% on average (Tab. 3), which still indicates a major contribution of
427 terrestrial organic matter to the Congo deep sea fan sediments.

428 The carbon isotopic composition remains also remarkably constant with a range of
429 $\delta^{13}\text{C}_{\text{org}}$ between -23.8 and -27.1 ‰ (Fig. 4) and an mean-value around -26 ‰ (Tab. 2). Such
430 values illustrate the dominant influence of organic matter inherited from plants with C₃
431 photosynthetic pathway and are in the same range of the particulate organic matter measured
432 in the Congo River ($\delta^{13}\text{C}_{\text{org}} = -26.7 \pm 0.4$ ‰, Mariotti et al., 1991; Holmes et al., 1996). If
433 we assume that $\delta^{13}\text{C}_{\text{org}}$ of marine organic matter is -21 ‰ for that part of the equatorial
434 Ocean (Tyson, 1995), and if the detrital end-member presents a mean $\delta^{13}\text{C}_{\text{org}} = -26.7$ ‰ as
435 reported by Mariotti et al. (1991), the F_{ter} values calculated in the studied cores would
436 indicate that 93% of the organic matter derives from the detrital source (Tab. 3). This
437 assumption is probably not fully valid, because terrigenous organic matter fraction is more
438 resistant than the marine fraction. Consequently this terrigenous input, although important, is
439 probably overestimated.

440 The relationship between total N (TN) and TOC reveals an intercept that is close to the
441 origin of the cross-plot (Fig. 8), consistent with the idea that most of the nitrogen is associated
442 with organic matter. If we assume an organic origin for nitrogen, the C/N ratios for the
443 studied area range between 10.7 and 15.5 (Tab. 2; Fig. 4). Such values are also indicative of a
444 mixture of marine phytoplankton (C/N~6.7 for Redfield ratio) and terrigenous sources,
445 which contain lower nitrogen than marine organic matter. The almost constant average C/N
446 ratio (~13) in the different studied cores would require that the relative proportion of these
447 two sources remain constant.

448 Molar C/N ratios of samples and end members are often used in linear mixing
449 equations to estimate the fraction of terrestrially derived organic carbon in sedimentary
450 environments. Several authors have shown that this calculation actually yields the fraction of
451 terrestrially derived organic nitrogen (Perdue and Koprivnjak, 2007 and references therein).
452 Because terrestrial organic matter is relatively depleted in nitrogen, the fraction of terrestrially

453 derived organic carbon has been seriously and systematically underestimated by this
1 454 misinterpretation of C/N mixing lines. Only the mixing equation based on N/C yields the true
2
3 455 fraction of terrestrially derived organic carbon.
4

5 456 We choose N/C ratios of 0.0653 and 0.142 as end-members for terrestrial and marine
6
7 457 sources, Xter and Xmar respectively. The Xter value chosen here is derived from the C/N
8
9 458 ratio (15.3) reported by Mariotti et al. (1991) for suspended particulate organic matter in the
10
11 459 load of the Congo River near its estuary, whereas the marine end-member is close to the
12
13 460 reverse of the C/N for Redfield ratio. Taking these values, the organic matter preserved in
14
15 461 sediments from the levees is clearly dominated by terrestrial organic matter which represents
16
17 462 almost 85 % of the preserved organic carbon (Tab. 3).

18 463 As $\delta^{13}\text{C}_{\text{org}}$ and N/C ratio, the nitrogen isotopic composition of sedimentary organic
19
20 464 matter ($\delta^{15}\text{N}$) has the potential to provide information on the source of organic matter to the
21
22 465 ocean (Calvert et al., 2001). $\delta^{15}\text{N}$ records the isotopic composition of the substrate (nitrate,
23
24 466 ammonium or dinitrogen) and the fractionation between the two isotopes ^{14}N and ^{15}N that
25
26 467 occurs during photosynthetic pathways so that $\delta^{15}\text{N}$ will depend on the relative utilisation of
27
28 468 the nitrogen source (Altabet and François, 1994). Since nitrate and atmospheric dinitrogen
29
30 469 have different isotopic signature (respectively $\sim 5\text{‰}$ and 0‰) and are the main sources of
31
32 470 nitrogen respectively for marine and terrestrial plants, the nitrogen isotopic signature of
33
34 471 marine plants and algae is heavier ($>4\text{--}5\text{‰}$) than for terrestrial plants ($<1\text{‰}$). Source
35
36 472 identification can be complicated in oceanic sedimentary systems when bacterial
37
38 473 denitrification occurs in oxygen-depleted waters or when dinitrogen fixation occurs in oceanic
39
40 474 waters. However, these processes are negligible in our area off Congo (see Holmes et al.,
41
42 475 1996). Finally, the same conclusion may be inferred from the nitrogen isotopic ratios ($\delta^{15}\text{N}$
43
44 476 around 5.5‰) which indicate a mixture of marine plants and C3 plants (Fig. 9). The terrestrial
45
46 477 fraction deduced from $\delta^{15}\text{N}$ data represents around 44% of the total organic matter (Tab. 3).

47 478
48 479 This inference for a dominance of land-derived organic matter in levee facies from the
49
50 480 Congo fan, based on low $\delta^{13}\text{C}_{\text{org}}$ and HI-values, is in conflict with the nitrogen isotope values
51
52 481 which are too heavy (<15) for such a dominance. The nitrogen isotopic composition of
53
54 482 sedimentary organic matter in the deep-sea fan of Congo must be considered with caution. In
55
56 483 a previous study in the same area, Müller et al. (1994) and Holmes et al. (1996) reported
57
58 484 already $\delta^{13}\text{C}_{\text{org}}$ typical of a mixing between terrestrial and marine plants whereas $\delta^{15}\text{N}$ values
59
60
61
62
63
64
65

485 were close to a marine end-member. In addition, higher than expected $\delta^{15}\text{N}$ values were
1 486 reported in the Congo estuary (Holmes et al., 1996).

3 487
4
5 488 This apparent contradiction in source characterization between carbon isotopic
6
7 489 composition, N/C ratio and Rock-Eval, in one hand, and nitrogen isotopic ratios, in other
8
9 490 hand, is evidence that the marine organic matter contributes significantly to the organic
10
11 491 content of these sediments. As algal marine hydrogen-rich organic matter (Type II) is
12
13 492 oxidized, its hydrogen content decreases while its oxygen content increases, and it may take
14
15 493 on Rock-Eval characteristics of Type III organic matter. The fact that samples having high
16
17 494 TOC content show HI-value reaching 256 mg HC/g TOC supports this hypothesis and
18
19 495 suggests that the algal organic matter was deeply oxidized by microbial reworking. Finally,
20
21 496 optical investigations of palynofacies reveal high proportion of fluffy amorphous organic
22
23 497 matter (Fig. 5A) which is usually derived from phytoplanktonic sources (Tyson, 1995). The
24
25 498 quantification using HI-values underestimates the real contribution of the marine source to the
26
27 499 enrichment in organic matter.

28 500
29 501 The thermochemolysis of 9 samples provides another way to estimate the terrestrial
30
31 502 versus marine contribution to the organic matter. All chromatograms are similar to that shown
32
33 503 on Fig. 10; the main quantitative data are given in Table 4. Compound distributions are
34
35 504 dominated by fatty acid methyl esters (FAMES) and lignin degradation products: vanillic and
36
37 505 syringic acids and aldehydes, coumaric and ferulic acids, plus non lignitic pHO-benzoic acid
38
39 506 and aldehyde. FAME distributions are dominated by even carbon numbered FA from C₂₂ to
40
41 507 C₃₄, with a mode at *n*-C₂₄ (Fig. 10). These compounds are also accompanied by lower but still
42
43 508 notable proportions of odd-numbered *n*-alkanes from C₂₇ to C₃₁, with a predominance of *n*-
44
45 509 C₂₉ (Fig. 10). All these compounds are classically assumed to be typical components of higher
46
47 510 plants, the C₂₀₊ FAMES and the high molecular weight *n*-alkanes being common constituents
48
49 511 of aerial plants cuticular waxes. Relatively high proportions of syringic moieties (i.e. acid plus
50
51 512 aldehyde) over their vanillic counterparts (S/V = 0.3-0.61; Tab. 4) reveal that lignin originates
52
53 513 from Angiosperms, with a contribution from Gymnosperms being not to be excluded (Hedges
54
55 514 and Mann, 1979). Rather extensive lignin alteration is revealed by the predominance of
56
57 515 vanillic and syringic acids over the corresponding aldehydes [(Vac+Sac)/(Vald+Sald) = 1.74
58
59 516 to 2.56; Tab. 4), by the high contribution of acid moieties to the total lignin (Vac+Sac)/Ltot =

517 0.55 to 0.65; table 4) and also by very low proportions of coumaric and ferulic acids (data not
1 2 518 shown), these two compounds originally linked to the lignin backbone by labile ester bonds
3 519 being rather easily degraded during early diagenesis (Bourdon et al., 2000). The importance
4 520 of the terrestrial organic matter contribution to the sediments is also assessed by rather high
5 521 lignin and C₂₀₊ even-carbon numbered FAMES concentrations, amounting to 32-48 mg.g⁻¹
6
7 522 TOC and 5.7 -26.4 mg g⁻¹ TOC, respectively (table 4). For comparison, recent analysis of
8
9 523 Holocene peat by the same methods (Disnar et al., 2008) yielded lignin and C₂₀₊ FAME
10
11 524 concentrations of 4-20 mg.g⁻¹ TOC and 2-7 mg g⁻¹ TOC, respectively. The higher yields
12
13 525 obtained with Congo sediments is very probably due the loss of the more labile constituents
14
15 526 (e.g. polysaccharides), during diagenesis.

16
17
18 527 The presence of FAMES from C₁₆ and C₁₈ is noted in all chromatograms. Such compounds
19
20 528 are usually produced by both algae and higher plants but they are rapidly destroyed in aerial
21
22 529 condition and soils (Marseille et al., 1999). Then, in sediments they can be assumed to derive
23
24 530 from autochthonous (marine) production. Hopanoids components are ubiquitous in all
25
26 531 analyzed samples, although in very low proportion. This suggests a contribution of bacterial
27
28 532 biomass, which may have developed in soil as well as within marine sediments.

29 533
30
31 534 To summarize, the recent mud-rich sediments from the Congo deep-sea turbidite
32
33 535 system contain high amounts of organic matter, the origin of which is a mixture of terrestrial
34
35 536 higher-plant debris and deeply oxidized phytoplanktonic material. Although we have
36
37 537 evidence that both sources contribute to the organic matter sedimentation in the Congo deep-
38
39 538 sea fan, their relative importance cannot be precisely quantified. In any case, the terrestrial
40
41 539 fraction of the organic matter appears very important (at least 70-80%) especially for such
42
43 540 depths and distance from the coast. Similar proportion (60 %) of terrestrial organic matter was
44
45 541 recently reported in the sediments from the GeoB6518-1 core recovered by 962 m of water-
46
47 542 depth close to the canyon/upper channel-levees transition (Weijers et al., 2009). This
48
49 543 similarity in the proportion of terrestrial organic matter in both localities is surprising in that
50
51 544 the sampling sites are at very different depths and processes that allow the accumulation of
52
53 545 sediments on the edge of the canyon and along the middle part of channel-levees system are
54
55 546 quite different (Savoye et al., 2000). This suggests a homogeneous distribution of the
56
57 547 particulate organic matter delivered by the Congo River in the different parts of the deep-sea
58
59 548 fan.

5.2 Controls on the distribution and accumulation of organic matter in channel-levees

Turbidite emplacement is discontinuous and usually produces layers of sediment in which organic matter quantity, type and preservational state are heterogeneous (Cowie et al., 1995; Meyers et al., 1996; Watanabe and Akiyama, 1998; Lindblom and Järnberg, 2004; Saller et al., 2006; Caja and Permanyer, 2008). By contrast, in the levees from the Congo mud-rich deep-sea fan, the organic matter appears very homogeneous regardless of the scale.

556

At the scale of a turbiditic small sequence, the organic matter shows more or less a constant quantity (3 %) and quality according to the pyrolysis parameters HI and OI. This is mainly due to the fine-grain composition of the turbidite off Congo which are mainly made by clay and fine silt fractions (10 μm as median grain-size). As organic matter particles are less dense than minerals, they are mainly associated with fine-grain component of the sediment. Organic matter particles have larger size in sandy facies but they are less numerous; then the organic content is usually lower at the base of sandy turbidites. Because the sandy fraction is a minor component of the studied levees, the organic matter content is near constant from the base to the top of a single turbiditic bed. Although, turbiditic clays cannot easily be distinguished from hemipelagic clays in such fine mud-rich system, the latter have been analysed at least in several levels and they show changes neither in quantity nor in type of organic matter. This implies that the hemipelagic sedimentary flux has more or less a similar characteristic for organic matter than the turbiditic input or, at least, that the preserved organic matter from hemipelagic sedimentation finally achieves the same characteristics.

Indeed, Treignier et al. (2006) studied the organic matter content and composition of sediment trapped 30 m above the channel before and just after a turbiditic event, as well as the surficial sediment sampled nine months after the event at the same water depth (~ 4000 m) than our studied area.

This sediment contained 4.2 % TOC and showed a predominance of long-chain *n*-alcohols typical for higher plant waxes, in the free lipid extracts. Despite the predominance of these compounds in cuticular waxes, and especially over long chain fatty acids and *n*-alkanes, they were absent among the thermochemolysis products of the nine samples we analyzed (Fig. 10). This absence is undoubtedly due to the microbial degradation of these labile compounds during early diagenesis. Treignier et al. (2006) estimated a degradation constant value

581 comprised between 0.6 and 1.2 y^{-1} for the C₂₂₊ *n*-alcohols that is rather considerable. The fate
1 582 of these compounds fully illustrates the considerable changes that can affect molecular
2 583 signatures during sedimentation and diagenesis and the importance of the choice of markers
3 584 used for assessing the origin and relative importance of original organic matter inputs to
4 585 sediments.
5 586

10 587 The quantity of organic matter is near constant in the transect located at 700 km from
11 588 the apex of the canyon (KZAI 04-05) compared to the transect located 150 km downstream
12 589 (KZAI 13-14), although the sediment accumulation rate increases by one order of magnitude
13 590 between these two areas (0.4 to 0.8 m/ka against 4.4 to 6.5 m/ka; Savoye et al., 2009).
14 591 However, these sedimentation rates are both important for deep-sea environments. Such
15 592 values indicate that, despite long distance transportation and/or deposition at rather great
16 593 water depth, sediment emplacement occurred rapidly which is a suitable condition for organic
17 594 matter preservation. Although the difference in the channel depth (140 m at KZAI 04-05 site
18 595 and 90 m at KZAI 14-15 site) generates ten times more spillovers downstream (Savoye et al.,
19 596 2009), the near constant quantity of organic matter suggests that the composition of the
20 597 spillovers of the channelized flows, where organic matter, clay minerals and silts are carried
21 598 in suspension, have a more or less similar composition in these different type of particles and
22 599 that in the channelized flow, between 90 m and 140 m height (50 m thickness), the turbulence
23 600 does not generate a significant segregation of organic particles. As the lithology of sediments
24 601 does not change a lot between the two areas, this assumption seems valid.

25 602 More surprising is the fact that changes in sediment accumulation rates do not imply
26 603 changes in the quality of the preserved organic matter. Usually, low sedimentation rates
27 604 determine a longer residence time of the organic particles in the oxygenated zone near the
28 605 water-sediment interface and consequently the organic matter is more easily remineralised.
29 606 On the contrary, high sedimentation rate led to a better preservation of organic particles. Here
30 607 the organic matter quality parameters (HI, OI, C/N, $\delta^{13}\text{C}_{\text{org}}$ and $\delta^{15}\text{N}$) appear very constant
31 608 along both the upstream and downstream transect.

32 609 This may be due to the fact that terrestrial organic particles, which are the main
33 610 component of the organic matter in Congo deep sea fan sediments, are more resistant than
34 611 marine organic matter. Marine organic matter may represent 40% of the preserved organic
35 612 matter but is also deeply and rapidly altered after deposition as shown by Treignier et al.
36
37
38
39
40
41
42
43
44
45
46
47
48
49
50
51
52
53
54
55
56
57
58
59
60
61
62
63
64
65

613 (2006) on the *n*-alcohol fraction. Thus, changes in marine contribution during settling have
1 614 little impact on the final composition of the organic matter of the sediment. It seems that after
2 615 its deposition, the organic mixture of terrestrial and marine particles is homogenised by
3 616 oxidative alteration and exhibits constant quality parameters.
4
5
6

7 617 A minor change is noted, however, in the HI and OI values with the distance from the
8
9 618 channel. Samples from cores KZAI 05 and 14 which are located closer to the channel display
10
11 619 higher HI- and lower OI-values compared to samples from cores KZAI 04 and 13 which are
12
13 620 500 to 5000 m separated from the counterpart. The changes are minor ($\Delta = -40$ mg HC/g
14
15 621 TOC for HI and $+40$ mg CO₂/g TOC for OI) but significant if we consider the distribution of
16
17 622 analysed samples on a HI-OI diagram (Fig. 11). Moreover, the dispersion of samples is more
18
19 623 important in the IH-IO diagram in cores located far from the channel. This is maybe the
20
21 624 indication that changes in accumulation rates have already a little impact on the quality of
22
23 625 organic matter.
24

25 626

25 627 **5.3 Implication for deep-sea petroleum source rocks analogs**

27 628 TOC is the primary parameter of source rock appraisal, with a threshold of 1 wt% at
28
29 629 the immature stage for potential source rocks. With an average TOC value which largely
30
31 630 exceeds this threshold, the fine-grained turbiditic sediments in the Congo deep-sea fan could
32
33 631 be regarded as good future gas-prone source rocks. Mean petroleum potential range between 4
34
35 632 and 4.7 kg HC per t rock and are mainly gas-prone as the organic matter is primarily of
36
37 633 terrestrial origin.

38 634 The shaly levees are the main sedimentary facies which built the present-day Congo
39
40 635 deep sea fan. The volume of potential source rock is here very important, especially if we
41
42 636 consider their proximity to the sandy reservoirs located in the channel filling. Such organic-
43
44 637 rich facies may also a source for biogenic gas, which is not yet fully characterized. Methane-
45
46 638 rich vents are numerous in the Congo deep sea fan and the degassing of studied cores has
47
48 639 been noted on board the research vessel just after their recovery.

49 640 Fossil analogs of the present-day deep sea fan are distributed along the Atlantic
50
51 641 passive margins throughout the geological times, especially in the Congo-Angola basin.
52
53 642 Ancient deep-sea fans are now buried and such facies may be regarded as contributors to the
54
55 643 regional petroleum systems. A recent study of the Oligocene succession off Angola
56
57
58
59
60
61
62
63
64
65

644 demonstrates the petroleum potential of deep-sea claystones deposited as levee facies (Disnar
1 645 et al., in press).

3 646

5 647 **5.4 Implication for the global carbon cycle**

7 648 The transfer of carbon from land to sea has been recognized as an important pathway
8
9 649 in the global carbon cycle (Milliman, 1991; Burdige, 2005). Rivers play a major role and
10
11 650 transport most of the ~500 Tg per year of organic carbon carried from land to the global ocean
12
13 651 (Spitzky and Ittekkot, 1991). One critical aspect in the ocean carbon budget is the particulate
14
15 652 export flux from the coastal zone to the open ocean (Biscaye and Andersson, 1994; Goni et
16
17 653 al., 1997; Hedges et al., 1997; Andersson and Mackenzie, 2004; Dagg et al., 2004). Several
18
19 654 programs have addressed this question on different types of oceanic margin and have shown
20
21 655 the diversity of the modes of transfer (i) in nature with terrestrial versus marine carbon, (ii) in
22
23 656 space with canyons playing a major role in channelling the particulate flux in some places,
24
25 657 (iii) in time with storms, instabilities, current surge playing a significant role in transporting
26
27 658 particles and carbon from the shelf to the slope and open ocean.

27 659 In the case of the Congo deep-sea fan, the main part of the sedimentary load, including
28
29 660 organic matter, is transported directly from the river mouth to the deep-sea because the
30
31 661 canyon starts within the estuary. Our results indicate that high concentration of organic matter
32
33 662 (3% on average) is preserved in the shaly facies developed all along the lower channel/levee
34
35 663 systems. These facies are the main deposits through time, as channel sandy facies represent
36
37 664 only 20% on seismic profiles (Droz et al., 1996; Savoye et al., 2000). Thus, huge amount of
38
39 665 organic matter is preserved in the deep-sea fan system of the Congo.

40 666 Anka and Séranne (2004) estimate the volume of ancient fan related to the Congo River from
41
42 667 Oligocene to Present to a minimum of $0.7 \cdot 10^6 \text{ km}^3$. Taking an average of 3% of Corg and
43
44 668 1500 kg/m^3 for the density of dry sediment, we may calculate that $3 \cdot 10^{13}$ tons of carbon are
45
46 669 stored in that part of the Atlantic margin.

47 670 If we assume that the present-day delivery of particulate organic matter by the Congo River (1
48
49 671 mg C/L and a mean flow around $50\,000 \text{ m}^3/\text{s}$) was constant through time and that this
50
51 672 particulate organic flux was totally preserved in the sediment of the margin, we calculate that
52
53 673 $5.4 \cdot 10^{13} \text{ t}$ of carbon should be stored since 34 Ma. Despite our roughly assumptions, both
54
55 674 estimations are in the same range and the magnitude is probably correct.

56 675

1
2
3
4
5
6
7
8
9
10
11
12
13
14
15
16
17
18
19
20
21
22
23
24
25
26
27
28
29
30
31
32
33
34
35
36
37
38
39
40
41
42
43
44
45
46
47
48
49
50
51
52
53
54
55
56
57
58
59
60
61
62
63
64
65

676 The Congo deep-sea turbiditic system is one of the largest in the world still affected by
1 677 turbidite sedimentation during the interglacial high sea-level (Savoye et al., 2000). Such a
2
3 678 phenomenon is unique along the present-day African margin as most of the canyons are not
4
5 679 connected with the river. During the glacial periods, when sea-level was low, other huge
6
7 680 rivers, including the Amazon River, were directly connected to their submarine canyons and
8
9 681 carbon transfer from land to deep sea was much more higher than today. Indeed, the present-
10
11 682 day situation of the Congo River cannot be generalized to low seal-level period and further
12
13 683 studies are needed to evaluate the efficiency of such systems for the storage of terrestrial
14
15 684 organic matter into the deep ocean at that time.
16

685

18 686 **6. Conclusion**

687

22 688 The claystones and siltstones deposited in the lower channel/levees system of the
23
24 689 Congo deep sea fan are devoid of carbonate and contain a high proportion of organic matter,
25
26 690 with total organic carbon content around 3 wt%. This organic richness appears very
27
28 691 homogeneous at different scales, although smaller quantities are noted in more sand-rich
29
30 692 facies corresponding to the basal part of turbiditic event.

31 693 The identification and quantification organic carbon sources are difficult because
32
33 694 several parameters influence the bulk and molecular characteristics of the preserved organic
34
35 695 matter. Hydrogen Index values, carbon isotopic ratios and molecular data, all indicate a strong
36
37 696 influence from the detrital source, with proportion as high as 90%. C/N ratios and nitrogen
38
39 697 isotopic ratios, on the contrary, suggest that marine contribution to the organic matter
40
41 698 sedimentation may represent up to 40 %. Although evidence exist that both sources contribute
42
43 699 to the organic matter sedimentation in the Congo deep-sea fan, their relative importance
44
45 700 cannot be precisely quantified. In any case, the terrestrial fraction of the organic matter
46
47 701 appears very important (at least 60%) for such depth and distance from the coast.

47 702 The quantity and quality of organic matter is near constant in cores located at 700 km
48
49 703 from the apex of the canyon compared to cores located 150 km downstream, although the
50
51 704 sediment accumulation rate increases by one order of magnitude between these two areas.
52
53 705 This suggests that the spillovers of the channelized flows, where organic matter, clay minerals
54
55 706 and silts are carried in suspension, have a more or less similar composition in these different
56
57 707 types of particles. Change in accumulation rates has already a little impact on the quality of
58
59
60
61
62
63
64
65

708 organic matter, as higher plant and soil organic matter particles, which seem to be dominant,
1
2 709 are more resistant than marine organic matter.

3 710 With a TOC content of 3% and petroleum potential around 4.5 kg HC per t rock, the
4
5 711 fine-grained turbiditic sediments in the Congo deep-sea fan could be regarded as good future
6
7 712 gas-prone source rocks. Analogs of the present-day deep sea fan are distributed along the
8
9 713 Atlantic passive margins throughout the geological times, and should be considered as
10
11 714 potential source rocks for the deep offshore realm.

12 715 Finally, the Congo deep-sea fan is a major conveyor of organic carbon to the deep
13
14 716 Atlantic Ocean in the present-day high sea-level situation. This system where the canyon is
15
16 717 connected to the estuary can be generalized to other deep sea fans during low sea-level
17
18 718 periods. Further studies are needed to evaluate the efficiency of such systems for the storage
19
20 719 of terrestrial organic matter into the deep ocean.

21
22 720
23
24
25
26
27
28
29
30
31
32
33
34
35
36
37
38
39
40
41
42
43
44
45
46
47
48
49
50
51
52
53
54
55
56
57
58
59
60
61
62
63
64
65

721 **Acknowledgements**

1 722 The present study was funded by the GDR Marges Program. We acknowledge TOTAL
2
3 723 Company for the permission to use core material. We acknowledge Marielle Hatton, Didier
4
5 724 Kéravis and Florence Savignac for their analytical help and Alexandre Lethiers for drawings.
6
7 725 We are also grateful to Phil Meyers and an anonymous reviewer for constructive comments.
8

9 726

10
11
12
13
14
15
16
17
18
19
20
21
22
23
24
25
26
27
28
29
30
31
32
33
34
35
36
37
38
39
40
41
42
43
44
45
46
47
48
49
50
51
52
53
54
55
56
57
58
59
60
61
62
63
64
65

727 **References**

- 1
2 728
3
4 729 Altabet M., François R., 1994. Sedimentary nitrogen isotopic ratio as a recorder for surface
5 730 ocean nitrate utilization. *Global Biogeochem. Cycles* 8, 103-116.
6
7 731 Anka Z., Séranne M., 2004, Reconnaissance study of the ancient Zaire (Congo) deep-sea fan
8
9 732 (ZaiAngo Project). *Mar. Geol.*, 209, 223-244.
10
11 733 Andersson A.J., Mackenzie F.T., 2004. Shallow-water oceans: a source or sink of
12 734 atmospheric CO₂? *Front. Ecol. And Env.*, 2, 348-353.
13
14 735 Babonneau, N., Savoye, B., Cremer, M., Klein, B., 2002. Morphology and architecture of the
15 736 present canyon and channel system of the Zaire deep-sea fan. *Mar. Petrol. Geol.* 19,
16 737 445-467.
17
18 738 Béhar F., Beaumont V., De B.Penteado H.L., 2001, Rock-Eval 6 Technology: Performances
19 739 and Developments. *Oil & Gas Science and Technology – Rev. IFP*, 56, 2, 111-134.
20
21 740 Berger W.H., 1989. Global maps of ocean productivity. In Berger W.H., Smetacek V.S.,
22 741 Wefer G. (Eds.), *Productivity of the Ocean: Present and Past*. Wiley-Interscience, New
23 742 York, 429–455.
24
25 743 Biscaye, P.E., Andersson, R.F., 1994. Fluxes of particulate matter on the slope of the southern
26 744 Middle Atlantic Bight: SEEP-II. *Deep-sea Res.* 41, 459-509.
27
28 745 Bourdon S., Laggoun-Défarge F., Maman O., Disnar J.-R., Guillet B. Derenne S., Largeau C.
29 746 (2000). Organic matter sources and early diagenetic degradation in a tropical peaty
30 747 marsh (Tritrivakely, Madagascar). Implications for environmental reconstruction
31 748 during the Sub-Atlantic. *Org. Geochem.* 31: 421-438.
32
33 749 Burdige D.J., 2005. Burial of terrestrial organic matter in marine sediments; a re-assessment.
34 750 *Global Biogeochemical Cycles.* 19, 4, GB4011, doi:10.1029/2004GB002368.
35
36 751 Caja M.A., Permanyer A., 2008. Significance of organic matter in Eocene turbidite sediments
37 752 (SE Pyrenees, Spain). *Naturwissenschaften*, 95, 1073-1077.
38
39 753 Calvert S.E., Pedersen T.F., Karlin R.E., 2001. Geochemical and isotopic evidence for post-
40 754 glacial paleoceanographic changes in Saanich Inlet, British Columbia. *Mar. Geol.* 174,
41 755 287-305.
42
43 756 Cowie G.L., Hedges J.I., Prahl F.G., De Lange G.J., 1995. Elemental and major biochemical
44 757 changes across an oxidation front in a relict turbidite: An oxygen effect. *Geochimica et*
45 758 *Cosmochimica Acta*, 59, 1, 33-46.
46
47
48
49
50
51
52
53
54
55
56
57
58
59
60
61
62
63
64
65

- 759 Coynel, A., Seyler P., Etcheber H., Meybeck M., Orange D., 2005. Spatial and seasonal
1 760 dynamics of total suspended sediment and organic carbon species in the Congo River.
2
3 761 Global Biogeochem. Cycles 19, 4, 17 p. doi:10.1029/2004GB002335
4
- 5 762 Dagg, M., Benner, R., Lohrenz, S., Lawrence, D., 2004. Transformation of dissolved and
6
7 763 particulate materials on continental shelves influenced by large rivers: plume
8
9 764 processes. Contin. Shelf Res. 24, 833-858.
- 10
11 765 Deniau I, Disnar J.R., Baudin F., Houzay J.P., in press. Characterization of the organic matter
12
13 766 of the Oligocene (Chattian) turbiditic fine grained deposits, offshore Angola. Organic
14
15 767 Geochemistry, doi:10.1016/j.orggeochem.2009.11.004.
- 16 768 Dennielou, B., Jouanneau, J.-M., in press. Ages and duration of sedimentary objects and
17
18 769 sediment accumulation rates on the recent channel-levee and terminal lobes of the
19
20 770 Zaire deep-sea fan. In: N. Babonneau, A. Morash and B. Savoye (Editors), Key results
21
22 771 of the integrated study of the modern Zaire/Congo Fan (ZaiAngo Project). TOTAL.
- 23 772 Disnar J. R., Jacob J., Morched-Issa M., Lottier N., Arnaud F. (2008) Assessment of peat
24
25 773 quality by molecular and bulk geochemical analysis; application to the Holocene
26
27 774 record of the Chautagne marsh (Haute Savoie, France). Chemical Geology, 254 : 101–
28
29 775 112.
- 30
31 776 Droz L., Rigaut F., Cochonat P., Tofani R., 1996. Morphology and recent evolution of the
32
33 777 Zaire turbidite system (Gulf of Guinea). Geol. Soc. Am. Bull., 108, 253-269.
- 34 778 Espitalié, J., Deroo, G., Marquis, F. 1985. La pyrolyse Rock-Eval et ses applications. Partie I.
35
36 779 Rev. Inst. Fr. Pétrole, 40/5, 563-579.
- 37
38 780 Gervais A., Mulder T., Savoye B., Migeon S., Cremer M., 2001. Recent processes of levee
39
40 781 formation on the Zaire deep-sea fan : CR Acad. Sci., 332, 371-378.
- 41
42 782 Goni, M.A., Ruttenberg, K.C., Eglinton, T.I., 1997. Sources and contribution of terrigenous
43
44 783 organic carbon to surface sediments in the Gulf of Mexico. Nature 389, 275-278.
- 45 784 Hedges J.I., Mann D. C. (1979) The characterization of plant tissues by their lignin oxidation
46
47 785 products. Geochim. Cosmochim. Acta 43, 1803–1807.
- 48
49 786 Hedges J.I., Oades J.M., 1997. Comparative organic geochemistries of soils and marine
50
51 787 sediments. Org. Geochem., 27, 319-361.
- 52
53 788 Hedges, J.I., Keil, R.G., Benner, R., 1997. What happens to terrestrial organic matter in the
54
55 789 ocean ? Org. Geochem. 27, 195-212.
- 56
57
58
59
60
61
62
63
64
65

- 790 Heezen B.C, Menzies R.J., Schneider E.D, Ewing W.M., Granelli N.C.L., 1964. Congo
1 791 submarine canyon. *Am. Assoc. Petr. Geol. Bull.*, 48, 1126-1149.
- 3 792 Holmes E., Müller P.J., Schneider R.R., Segl M., Pätzold J., Wefer G., 1996. Stable nitrogen
4 793 isotopes in Angola Basin surface sediments. *Mar. Geol.* 134, 1-12.
- 7 794 Holtvoeth J., Kolonic S., Wagner T., 2005. Soil organic matter as an important contributor to
8 795 late Quaternary sediments of the tropical West African continental margin.
9 796 *Geochimica et Cosmochimica Acta*, 69, 8, 2031–2041.
- 12 797 Huc A.Y., Bertrand P., Stow D.A.V., Gayet J., Vandenbroucke M., 2001. Organic
13 798 sedimentation in deep offshore settings: the Quaternary sediments approach. *Mar.*
14 799 *Petrol. Geol.*, 18, 513-517.
- 18 800 Khripounoff, A., Vangriesheim, A., Babonneau, N., Crassous, P., Dennielou, B., Savoye, B.,
19 801 2003. Direct observation of intense turbidity current activity in the Zaire submarine
20 802 valley at 4000 m water depth. *Mar. Geol.* 194, 151-158.
- 23 803 Kinga-Mouzeo M., 1986. Transport particulaire actuel du fleuve Congo et de quelques
24 804 affluents : enregistrement quaternaire dans l'éventail détritique profond
25 805 (sédimentologie, minéralogie et géochimie), Ph.D. thesis, Univ. de Perpignan, France,
26 806 261 pp.
- 31 807 Lafargue, E., Marquis, F., Pillot, D., 1998, Rock-Eval 6 Applications in Hydrocarbon
32 808 Exploration, Production and Soils Contamination Studies. *Oil & Gas Science and*
33 809 *Technology– Rev. IFP*, 53, 4, 421-437.
- 36 810 Lindblom S., Järnberg U., 2004. Organic geochemistry of lipids in marine sediments in the
37 811 Canary Basin: Implications for origin and accumulation of organic matter. In R.J. Hill,
38 812 J. Leventhal, Z. Aizenshtat, M.J. Baedeker, G. Claypool, R. Eganhouse, M.
39 813 Goldhaber and K. Peters (Eds) *Geochemical Investigations in Earth and Space*
40 814 *Science: A Tribute to Isaac R. Kaplan*. The Geochemical Society, Publication n° 9,
41 815 409-423.
- 47 816 Mariotti A., Gadel F., Giresse P., Kinga-Mouzeo M., 1991. Carbon isotope composition and
48 817 geochemistry of particulate organic matter in the Congo River (Central Africa):
49 818 application to the study of Quaternary sediments off the mouth of the river. *Chem.*
50 819 *Geol.*, 86, 345-357.
- 54
55
56
57
58
59
60
61
62
63
64
65

- 820 Marseille F., Disnar J. R., Guillet B., Noack Y. (1999) n-Alkanes and free fatty acids in humus
1 821 and A1 horizons of soils under beech, spruce and grass in the Massif Central (Mont-
2 822 Lozère) France. *Eur. J. Soil Sci.*, 50 : 433-441.
- 3 823 Martins O., Probst J.L., 1991. Biogeochemistry of major African rivers: carbon and minerals
4 824 transport, in *Biogeochemistry of Major World Rivers*, edited by E.T. Degens, S.
5 825 Kempe, J.E. Richey, SCOPE, 42, 127– 156.
- 6 826 Meybeck M., Ragu A., 1996. River discharges to the oceans: an assessment of suspended
7 827 solids, major ions, and nutrients, environment information and assessment report, 250
8 828 pp., U.N. Environ. Programme, Nairobi.
- 9 829 Meyers P.A., Silliman J., Shaw T.J., 1996. Effects of turbidity flows on organic matter
10 830 accumulation, sulfate reduction, and methane generation in deep-sea sediments on the
11 831 Iberia Abyssal Plain. *Org. Geochem.* 25, 1-2, 69-78.
- 12 832 Migeon S., Savoye B., Babonneau N., Spy Andersson F-L., 2004. Processes of sediment-
13 833 wave construction along the present-day Zaire deep-sea meandering channel: role of
14 834 meanders and flow stripping. *J. Sedim. Res.*, 74, 4, 580-598.
- 15 835 Milliman, J.D., 1991. Flux and fate of fluvial sediment and water in coastal seas. In:
16 836 Mantoura, R.F.C., J-M. Martin, R. Wollast (Ed.), *Ocean margin processes in global
17 837 change*. J. Wiley and sons, Berlin, pp. 69-91.
- 18 838 Müller P.J., Schneider R.R., Ruhland G., 1994. Late Quaternary pCO₂ variations in the
19 839 Angola Current: evidence from organic carbon $\delta^{13}\text{C}$ and alkenone temperatures. In: R.
20 840 Zahn et al. (Eds.), *Carbon Cycling in the Glacial Ocean: Constraints on the Ocean's role
21 841 in Global Change*, NATO ASI. Ser. C, I 17, Springer, Berlin, 343-366.
- 22 842 N'kounkou R.R., Probst J.L., 1987. Hydrology and geochemistry of the Congo River system,
23 843 in *Transport of Carbon and Minerals in Major World Rivers*, vol. 64, edited by E. T.
24 844 Degens, S. Kempe, and W. B. Gan, *Mitt. Geol.-Paläont. Inst., Univ. Hamburg*, 483-
25 845 508.
- 26 846 Perdue M., Koprivnjak J.F.. 2007. Using the C/N ratio to estimate terrigenous inputs of
27 847 organic matter to aquatic environments. *Estuarine, Coastal and Shelf Science*, 73, 65-
28 848 72. Peters, K.E. 1986. Guidelines for evaluating petroleum source rock using
29 849 programmed pyrolysis. *American Association of Petroleum Geologists Bulletin*. 70,
30 850 318–329.

- 851 Piper D.J.W., 1978. Turbidite muds and silts on deep sea fans and abyssal plains. *In* Stanley
1 852 D.J, Kelling E. (eds). Sedimentation in submarine canyons, fans and trenches.
2
3 853 Stroudsburg, Pennsylvania, Dowden, Hutchinson & Ross, p. 163-176.
4
5 854 Saller A., Lin R., Dunham J., 2006. Leaves in turbidite sands: the main source of oil and gas
6
7 855 in the deep-water Kutei Basin, Indonesia. AAPG Bull., 90, 1585-1608.
8
9 856 Savoye, B., Babonneau, N., Dennielou, B., Bez M., 2009. Geological overview of the
10
11 857 Angola-Congo Margin, the Congo deep-sea fan and its submarine valleys. Deep Sea
12
13 858 Research, Part II: Topical Studies in Oceanography, 56, 2169-2182.
14
15 859 Savoye, B., Cochonat, P., Apprioual, R., Bain, O., Baltzer, A., Bellec, V., Beuzart, P.,
16 860 Bourillet, J.-F., Cagna, R., Cremer, M., Crusson, A., Dennielou, B., 2000. Structure et
17
18 861 évolution récente de l'éventail turbiditique du Zaire : premiers résultats scientifiques
19
20 862 des missions d'exploration Zaiango1 & 2 (marge Congo-Angola). C.R. Acad. Sci.
21
22 863 Séries IIA 331, 211-220.
23
24 864 Servain J., Picaut J, Merle J., 1982. Evidence of remote forcing in the equatorial Atlantic
25 865 Ocean. J. Phys. Ocean., 12, 457-463.
26
27 866 Spitzky A., Ittekkot V., 1991. Dissolved and particulate organic matter in rivers. *In* Mantoura
28
29 867 R.F.C.et al. (Eds) Ocean Margin Processes in Global Change, John Wiley, pp. 5 – 17.
30
31 868 Stow D.A.V., Huc. A.Y., Bertrand P., 2001. Depositional processes of black shales in deep
32
33 869 water. Mar. Petrol. Geol. 18, 491-498.
34
35 870 Tissot, B.P., Welte, D.H. 1984. Petroleum formation and occurrence. Springer, Berlin. 699 p.
36
37 871 Treignier C., Derenne S., Saliot A. 2006. Terrestrial and marine n-alcohol inputs and
38 872 degradation processes relating to a sudden turbidity current in the Zaire canyon. Org.
39
40 873 Geochem., 37, 1170-1184.
41
42 874 Tyson, R.V. 1995. Sedimentary organic matter: organic facies and palynofacies. Chapman &
43
44 875 Hall, London. 615 p.
45
46 876 van Bennekom A.J., Berger G.W., 1984. Hydrography and silica budget of the Angola Basin.
47 877 Neth. J. Sea Res., 17, 149-200.
48
49 878 Vangriesheim A., Krhipounoff A., Crassous P. 2009. Turbidity events observed in situ along
50
51 879 the Congo submarine channel. Deep-Sea Research, Part II: Topical Studies in
52
53 880 Oceanography, 56, 2208-2222, doi:10.1016/j.dsr2.2009.04.004
54
55 881 Voituriez B., Herbland A., 1981. Primary production in the tropical Atlantic Ocean mapped
56 882 from oxygen values of Equalant 1 and 2 (1963). Bull. Mar. Sci., 31, 853-863.
57
58
59
60
61
62
63
64
65

883 Watanabe H., Akiyama M., 1998. Characterization of organic matter in the Miocene
1 turbidites and hemipelagic mudstones in the Niigata oil field, central Japan. *Org.*
2
3 885 *Geochem.* 29, 1-3, 605-611.
4
5 886 Weijer J.W.H., Schouten S., Schefuss E., Schneider R.R., Sinninghe Damsté J.S., 2009.
6
7 887 Disentangling marine, soil and plant organic carbon contributions to continental
8
9 888 margin sediments: a multi-proxy approach in a 20,000 year sediment record from
10
11 889 Congo deep-sea fan. *Geochem. Cosmochem. Acta*, 73, 119-132.
12
13 890 Wetzel A., 1993. The transfer of river load to deep-sea fans: a quantitative approach. *AAPG*
14 891 *Bull.*, 77, 1679-1692.
15
16 892
17
18
19
20
21
22
23
24
25
26
27
28
29
30
31
32
33
34
35
36
37
38
39
40
41
42
43
44
45
46
47
48
49
50
51
52
53
54
55
56
57
58
59
60
61
62
63
64
65

893 **Captions of figures and tables**

1 894

2 895 Fig. 1. General map of central Africa and the Gulf of Guinea in eastern equatorial Atlantic
3 896 Ocean, showing the course of the Congo River, its main distributaries and its drainage area
4 (watershed), the surface and subsurface currents (open arrows: cold currents; black arrows:
5 897 warm currents), and highly productive areas (the latter modified from Schneider et al., 1994).

6 898

7 899
8 900 Fig. 2. Top: bathymetric map (contour interval: 100 m) showing the general morphology of
9 901 the Congo canyon and the modern meandering channel along the Congo fan. Limits of the
10 902 canyon, upper fan, channel/levee systems and lobes are from Babonneau et al. (2002). Studied
11 903 areas are located in the lower channel/levee systems. Bottom: Detailed bathymetric map
12 904 (contour interval: 10 m) and location of studied cores within the two studied areas, modified
13 905 after Gervais et al. (2001), Migeon et al. (2004).

14 906

15 907 Fig. 3. Top: line drawings of 3.5 kHz profiles showing the internal structures of the studied
16 908 levees and location of studied cores along these schematic cross-sections (Migeon et al. 2004
17 909 ; Gervais et al. 2001). Bottom: core logs showing the sediment grain-size changes and the
18 910 sampled interval along each core, redrawn after Migeon et al. (2004), Gervais et al. (2001)
19 911 and Migeon (2000).

20 912

21 913 Fig. 4. Vertical distribution of grain-size parameters (granulometric composition, median
22 914 grain-size), Total Organic Carbon (TOC, in weight %), Hydrogen Index (in mg HC/g TOC),
23 915 C/N and $\delta^{13}\text{C}_{\text{org}}$ (in ‰) of the four cores studied in the levee facies with a 20 cm-spacing.
24 916 Core location is shown on figs. 3 and 4.

25 917

26 918 Fig. 5. Microphotographs of palynofacies of the fine grained sediments of the levees from the
27 919 Congo deep sea fan near 4000 m-depth. a: Amorphous organic matter (AOM) having a fluffy
28 920 aspect. b: AOM containing small ligno-cellulosic debris. c: Structured phytoclast, apparently
29 921 derived from root cortex tissues. d: Partly-gelified ligno-cellulosic debris on which vegetal
30 922 fibre are still discernible. e: Opaque particle with corroded outlines on the right and small
31 923 piece of structurless phytoclast on the left. f: Spore.

32 924

33

34

35

36

37

38

925 Fig. 6. Vertical distribution of median grain-size (in μm), Total Organic Carbon (TOC, in
926 weight %), Hydrogen and Oxygen Indexes (in mg HC/g TOC and mg CO_2 /g TOC,
927 respectively) in several elemental turbiditic beds from cores KZAI 04, 14 and 15 with a 2 cm-
928 spacing. Core location is shown on figs 3 and 4.

929 A and B: type 1-bed, C and D: type 2-bed, E: type 3-bed, F: type 4-bed following the
930 nomenclature defined by Migeon et al. (2004).

931
932 Fig. 7. Kerogen type in the silty-clayey sediments of the lower channel/levee systems from
933 the Congo fan as defined by the cross-plot of TOC and pyrolysis S_2 parameters. Nearly all
934 samples are located in the domain of Type III organic matter which usually derives from
935 higher plant debris.

936
937 Fig. 8. Relationship between total organic carbon and total nitrogen for three core sediments
938 from the lower channel-levees system of the Congo fan. The linear regression line based on
939 all data points ($R^2=0.81$) is indicated by the dashed line.

940
941 Fig. 9. Kerogen type in the silty-clayey sediments of the lower channel/levee systems from
942 the Congo fan as defined by the cross-plot of $\delta^{13}\text{C}_{\text{org}}$ (in ‰) and $\delta^{15}\text{N}$ (in ‰). Here the
943 organic matter derives from a mixture of C3 land plants and marine algae.

944
945 Fig. 10. Example of partial reconstituted Total Ion Current (TIC) chromatogram of the
946 products of thermochemolysis with TMAH of sample from the silty-clayey sediments of the
947 lower channel/levee systems from the Congo fan (sample KZAI 05 – 540-541 cm). The
948 dominance of lignin-derived compounds (L), long-chain and odd-numbered n -alkanes, and
949 long-chain fatty acid methyl esters (FAMES) indicate the predominance of terrestrial organic
950 matter. Nevertheless, nC16:0 and nC18:0 FAMES may be interpreted as derived from algal
951 biomass whereas the presence of hopanoid testifies from a bacterial origin of some part of the
952 organic matter.

953 L = lignin derivatives and others phenolic compounds, all as Me ester and ethers (in
954 increasing elution order) : pHO-benzaldehyde, pHO-benzoic acid, vanillin, vanillic acid
955 (dominant), syringaldehyde, coumaric acid, syringic acid, ferulic acid.

956 Hopanoids : the first compound H30 is the regular hopane, the three following ones (H30-H32)
1 957 are hopanoic acids (as Me esters).

3 958

5 959 Fig. 11. van Krevelen diagram showing the homogeneity of the organic matter in the silty-
6
7 960 clayey sediments of the lower channel/levee systems from the Congo fan. The samples which
8
9 961 are more distant from the axis of the channel show lower HI-values and higher OI-values
10
11 962 indicating a little bit stronger oxidation effect.

13 963

14 964 Tab. 1. Location of the studied cores (Lat., Long., water-depth), penetration into the
15
16 965 sediments, length of studied interval and number of studied samples.

18 966

20 967 Tab. 2. Bulk inorganic and organic characteristics of the studied samples in each studied core.
21
22 968 Minimum, mean and maximum values are given for CaCO₃ (in %), TOC (in %), Hydrogen
23 969 Index (HI, in mg HC/g TOC), C/N, $\delta^{13}\text{C}_{\text{org}}$ (in ‰) and $\delta^{15}\text{N}$ (in ‰).

25 970

27 971 Tab. 3. Estimates of terrestrial organic matter fraction (in %) of the total organic matter in
28
29 972 marine sediments from KZAI cores based on the binary mixing models of different proxies.

31 973

33 974 Tab. 4 . Main data on lignin-derived products and on FAMES released by thermochemolysis

34 975 Sac, Sald & S = syringic acid, aldehyde and total, respectively

36 976 Vac, Vald & V = vanillic acid, aldehyde and total, respectively

38 977 Ltot = total lignin = S + V + (coumaric and ferulic acids)

40 978 *Compound concentrations in mg.g⁻¹TOC. Note that sample from core KZAI 15 corresponds
41
42 979 to a sandy facies from the channel.

43
44
45
46
47
48
49
50
51
52
53
54
55
56
57
58
59
60
61
62
63
64
65

Figure 1
[Click here to download high resolution image](#)

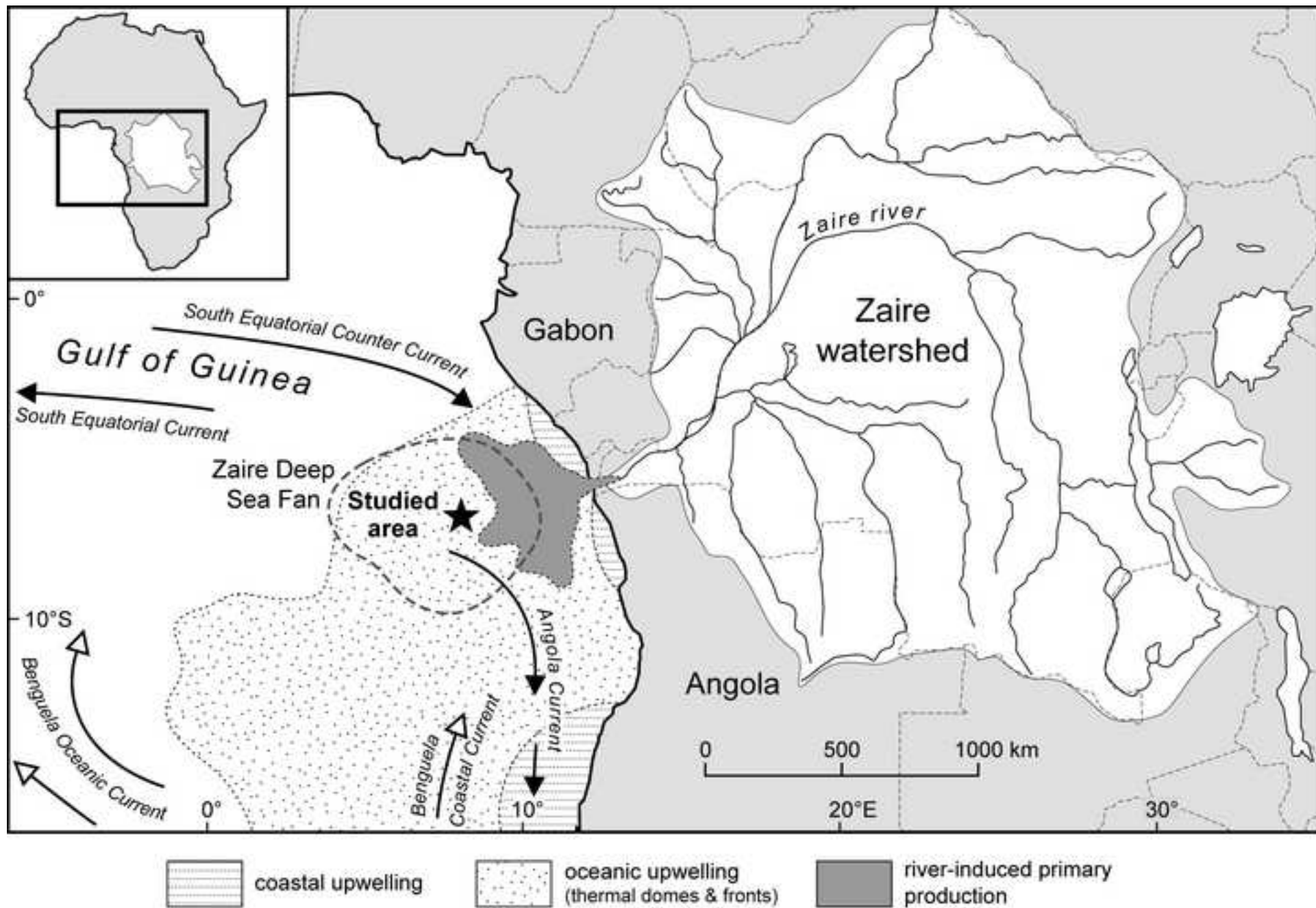


Figure 2
[Click here to download high resolution image](#)

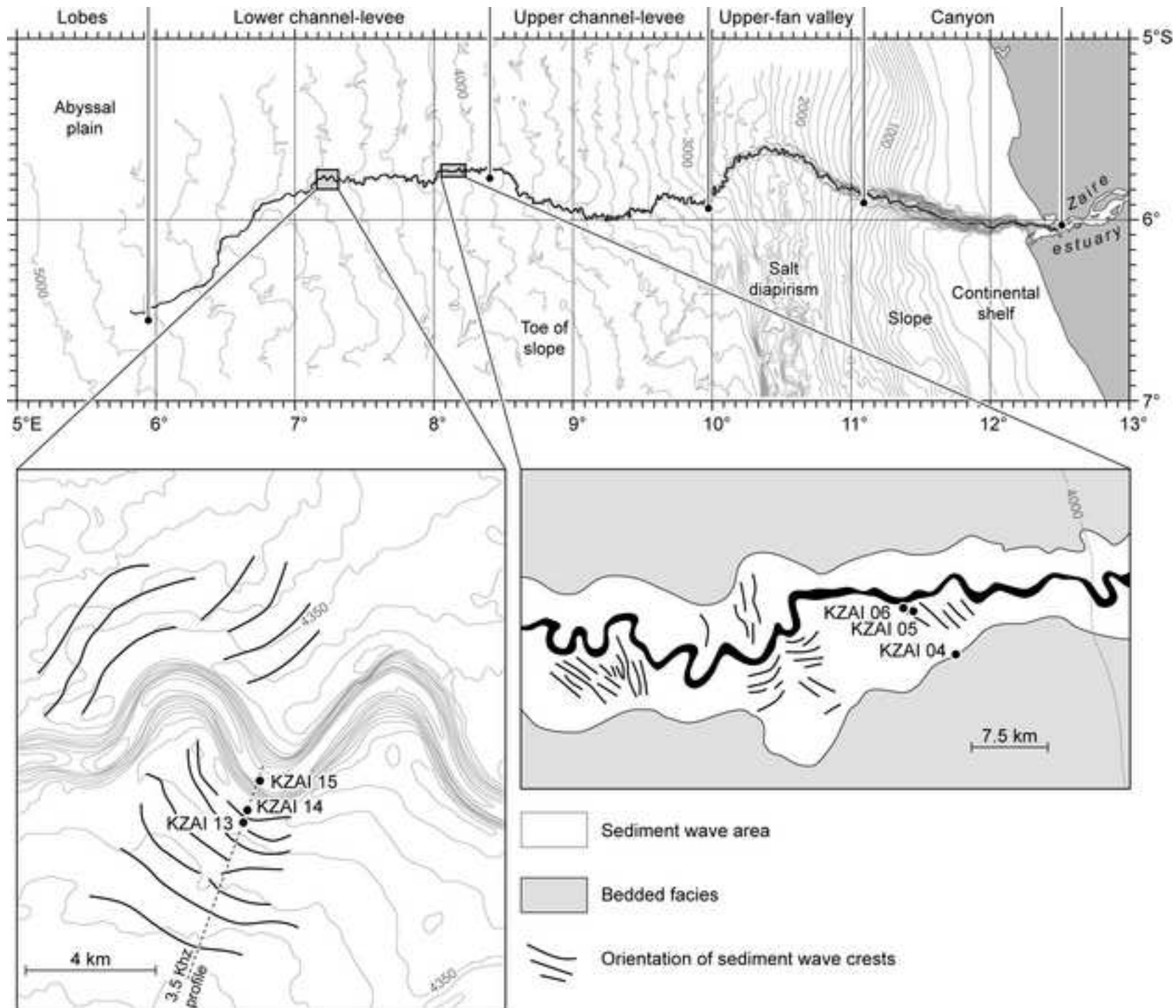


Figure 3
[Click here to download high resolution image](#)

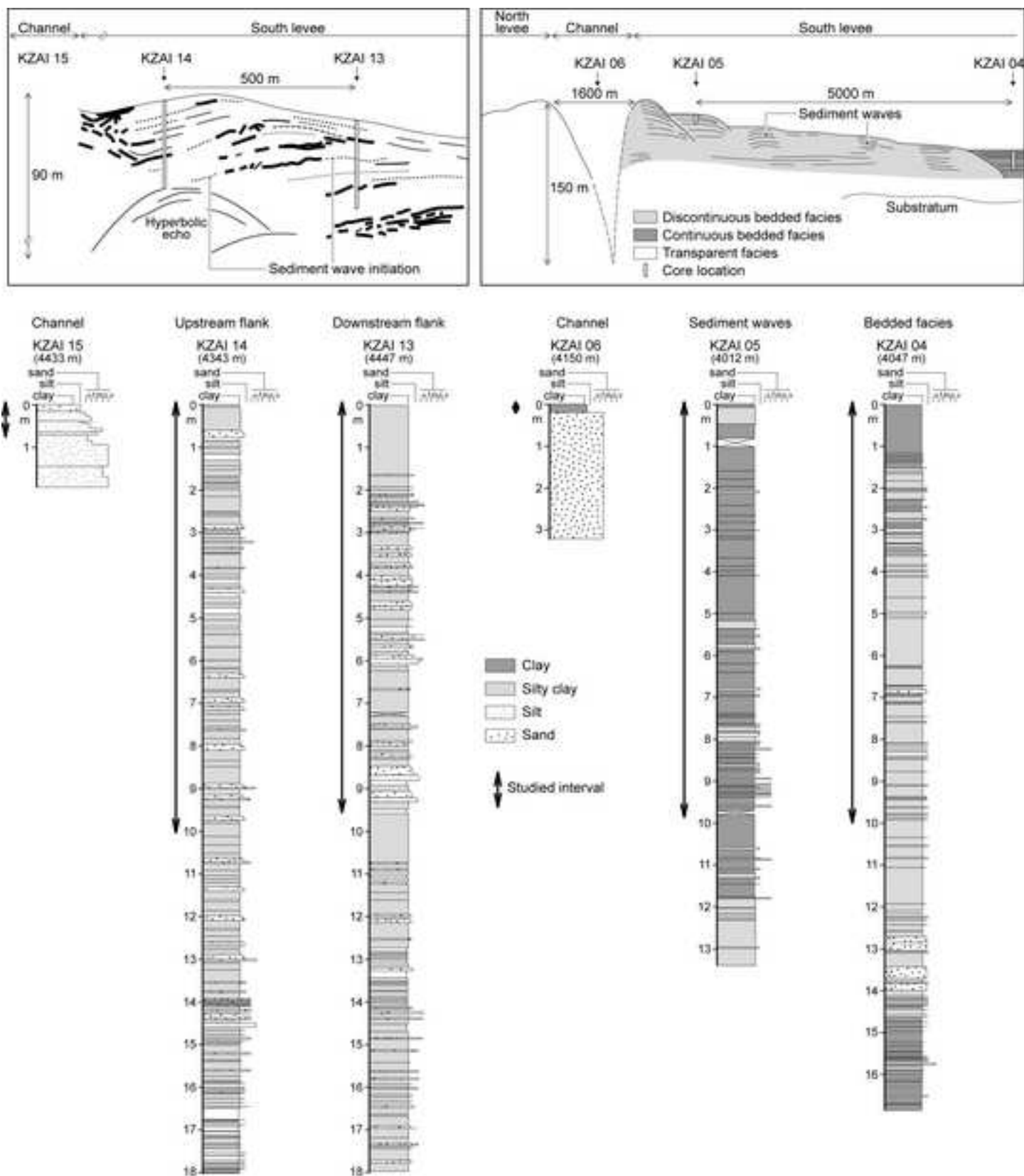


Figure 4
[Click here to download high resolution image](#)

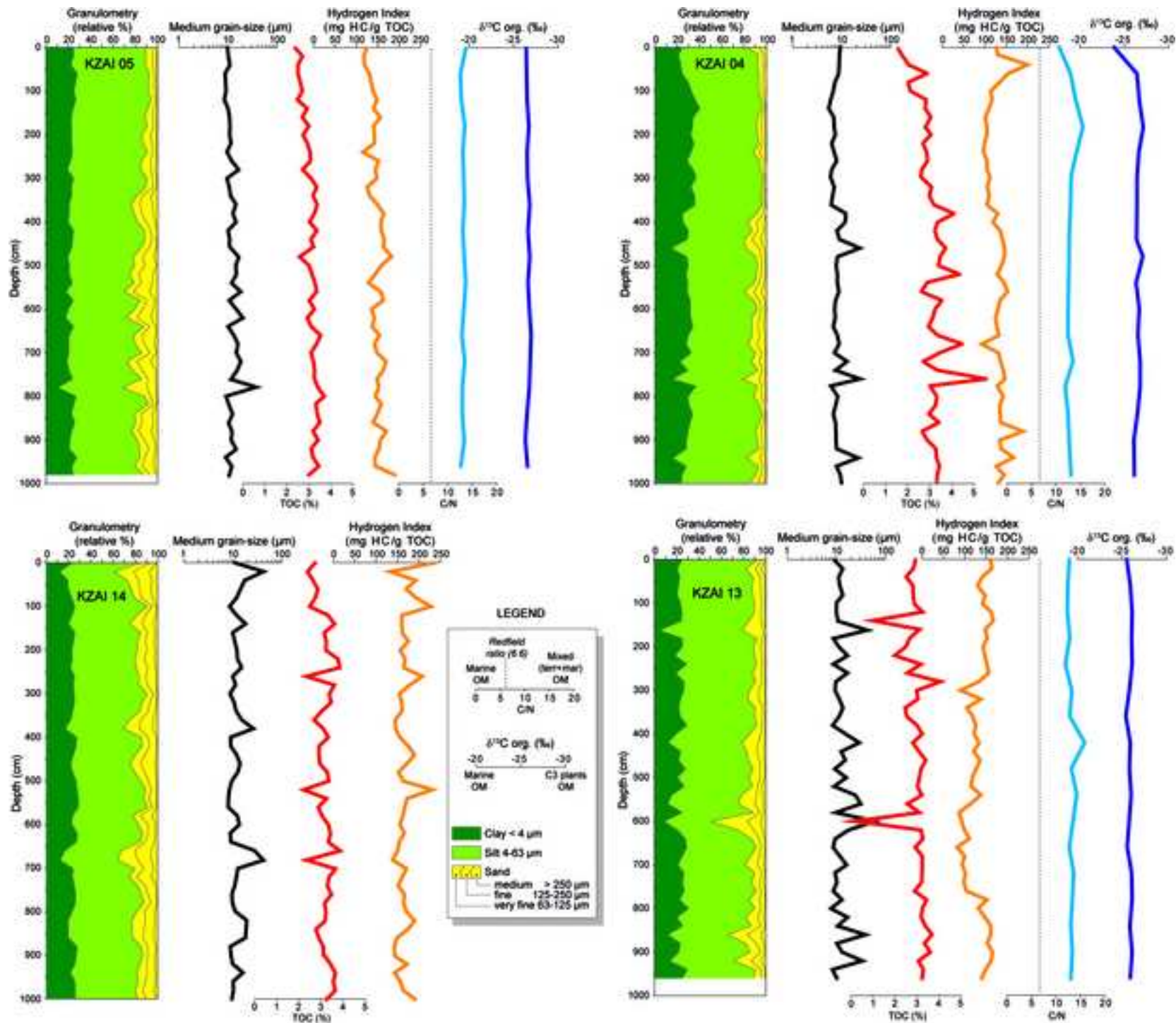


Figure 5
[Click here to download high resolution image](#)

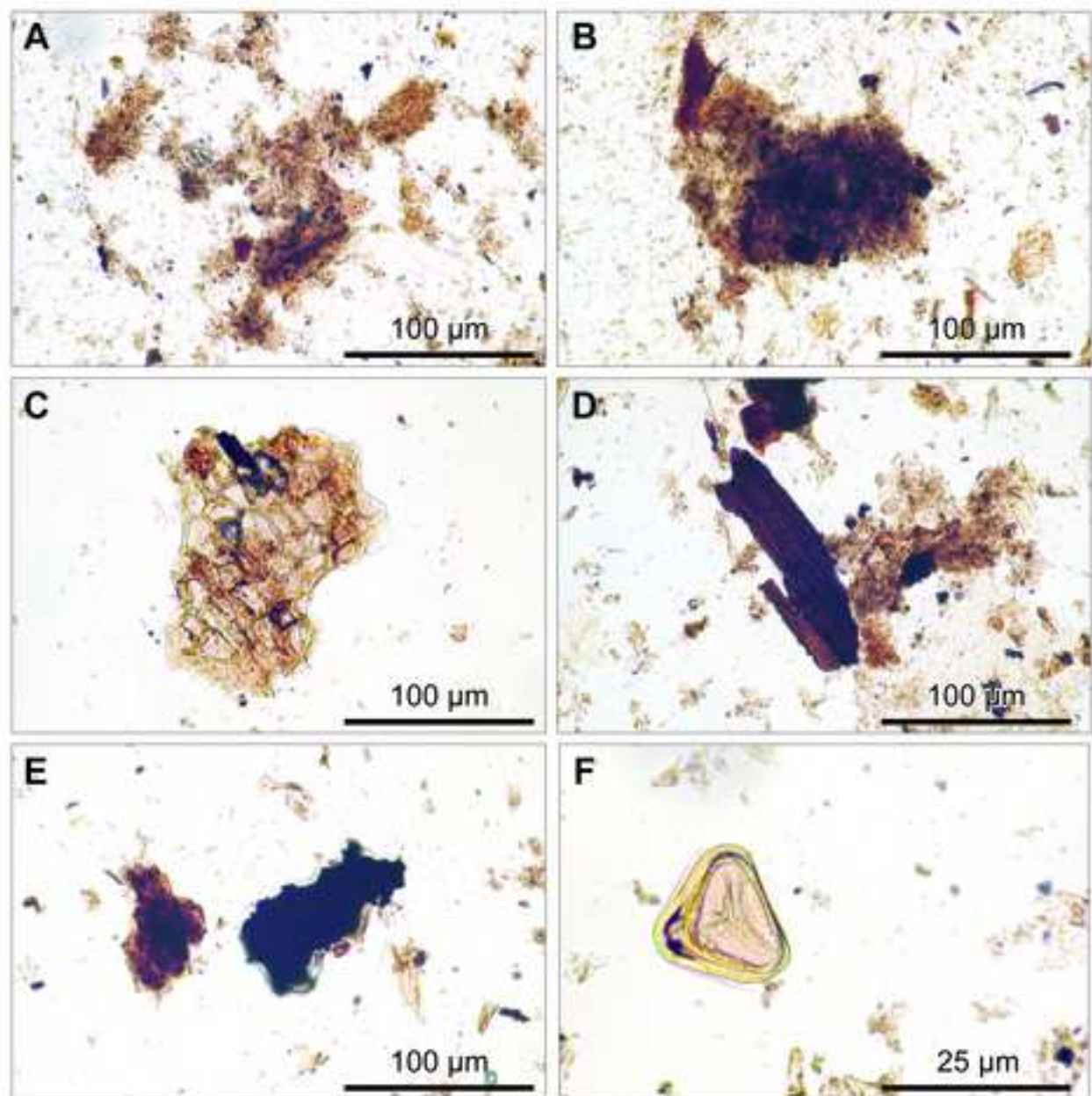


Figure 6
[Click here to download high resolution image](#)

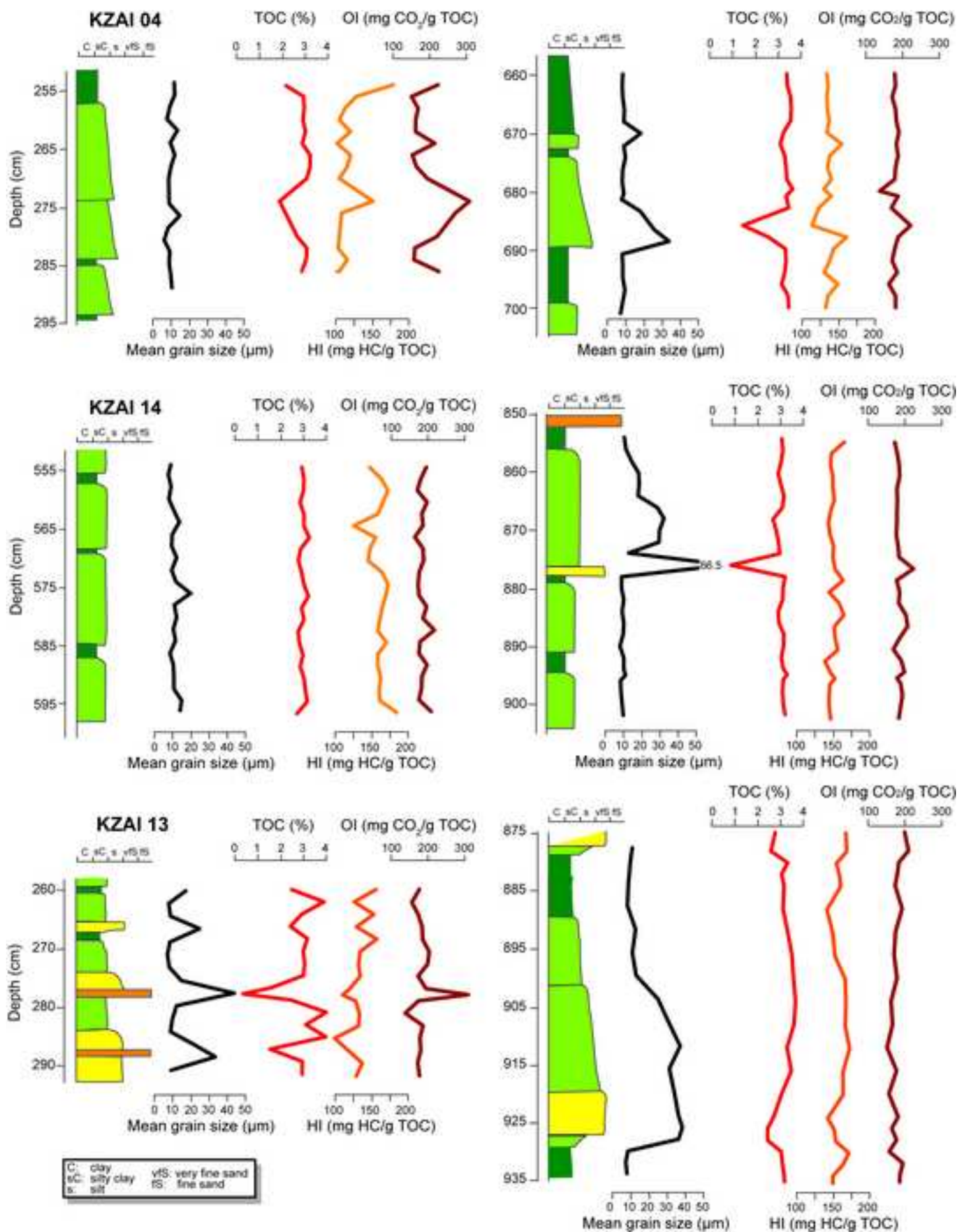


Figure 7
[Click here to download high resolution image](#)

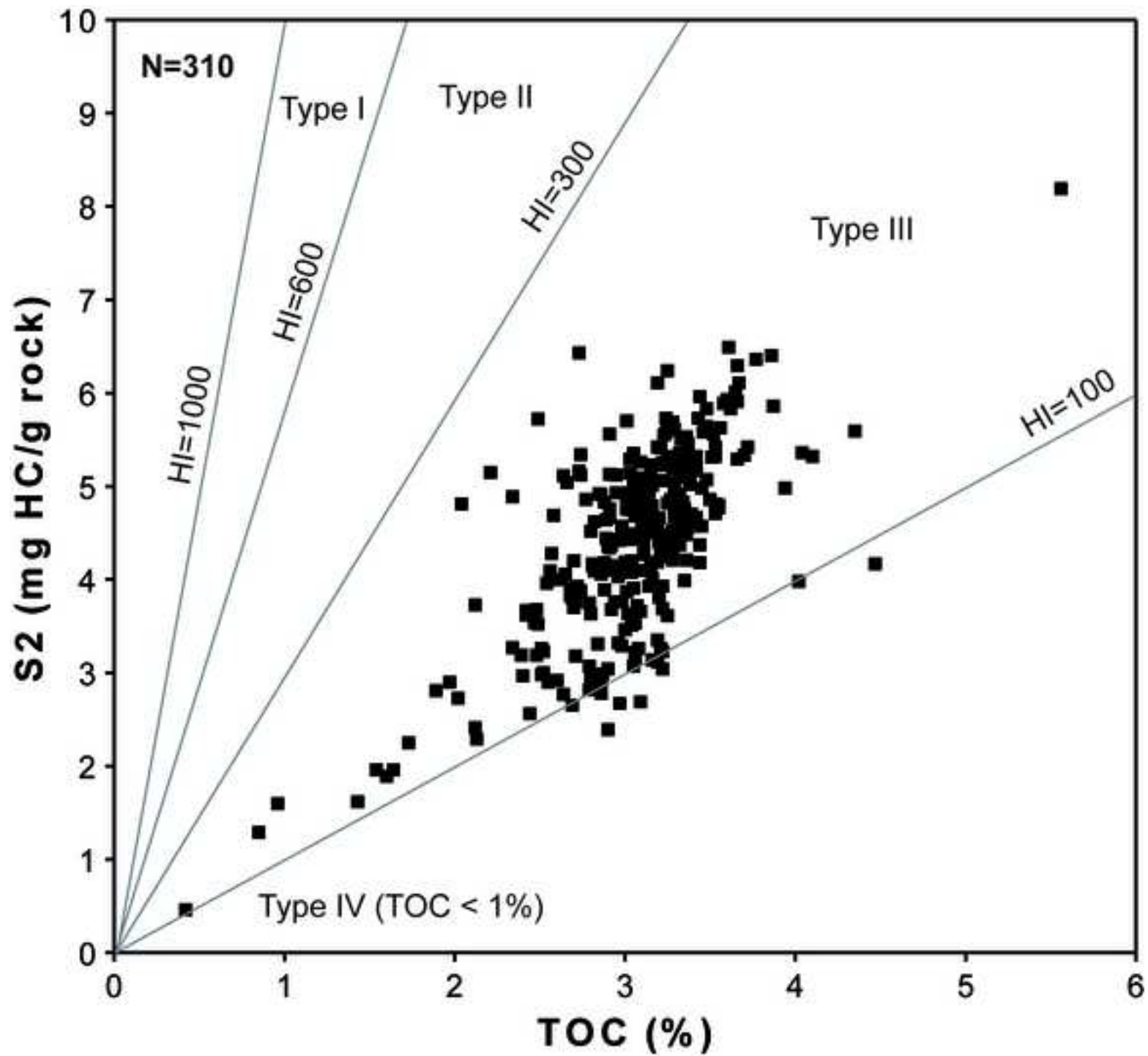


Figure 8
[Click here to download high resolution image](#)

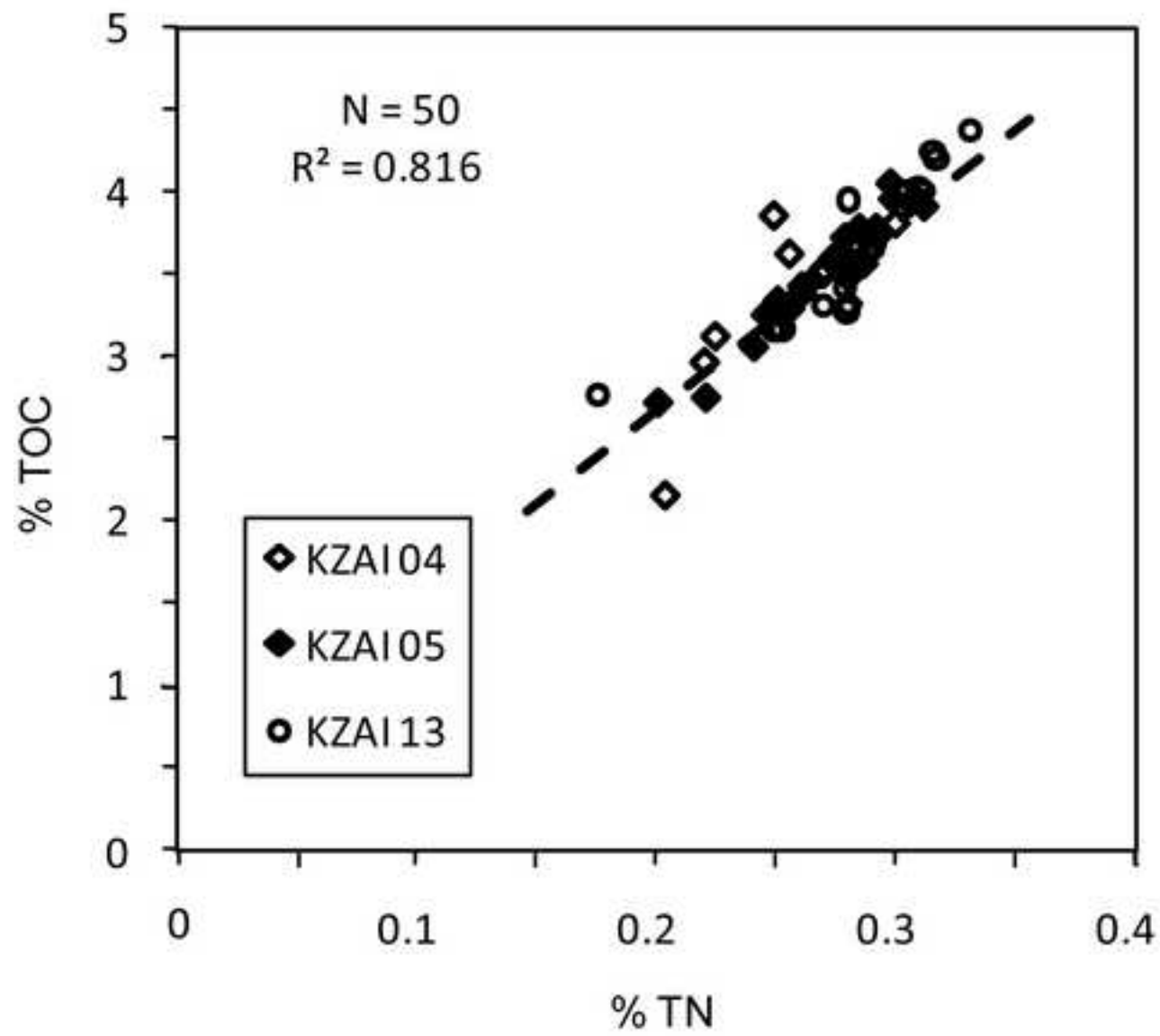


Figure 9
[Click here to download high resolution image](#)

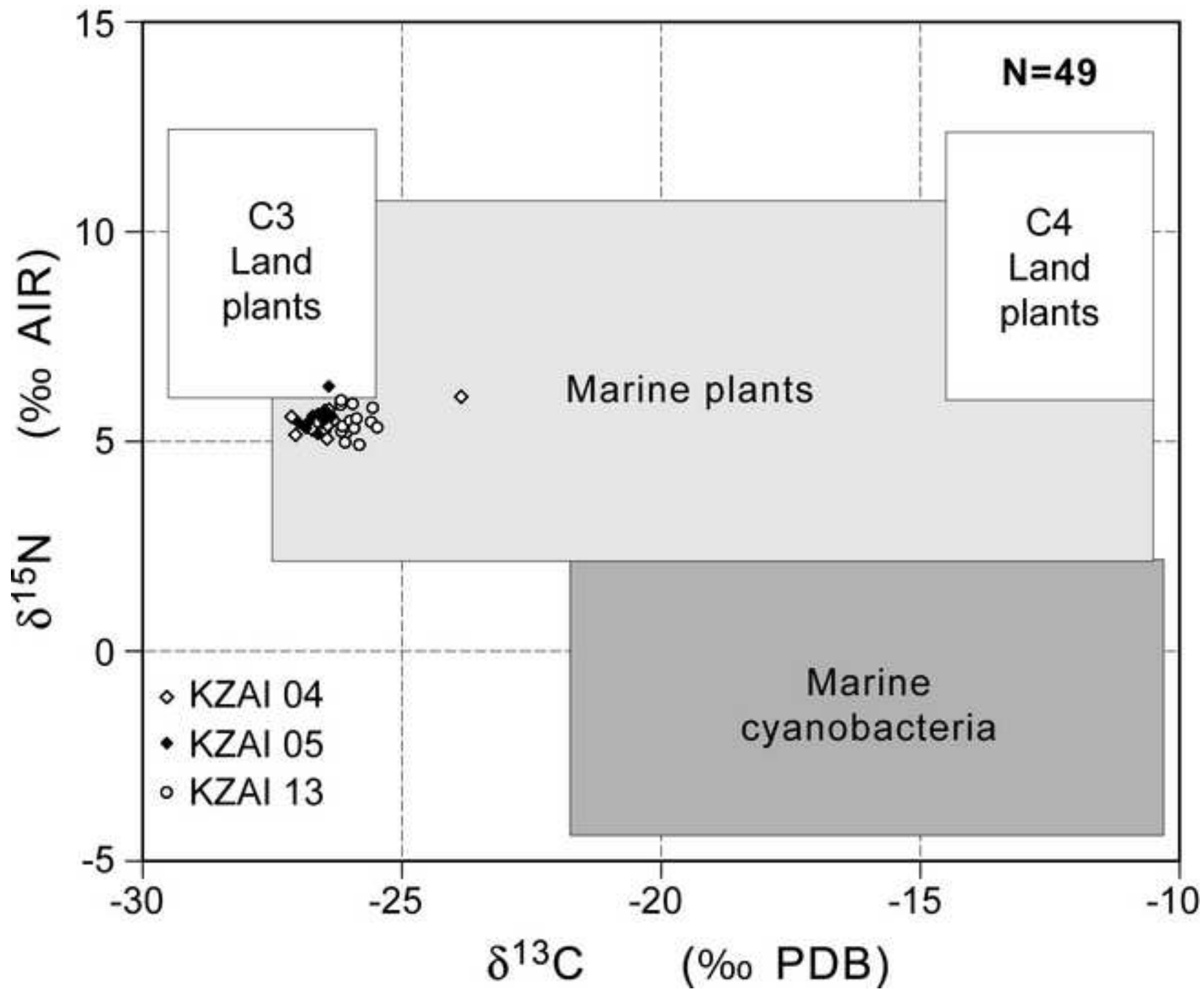


Figure 10
[Click here to download high resolution image](#)

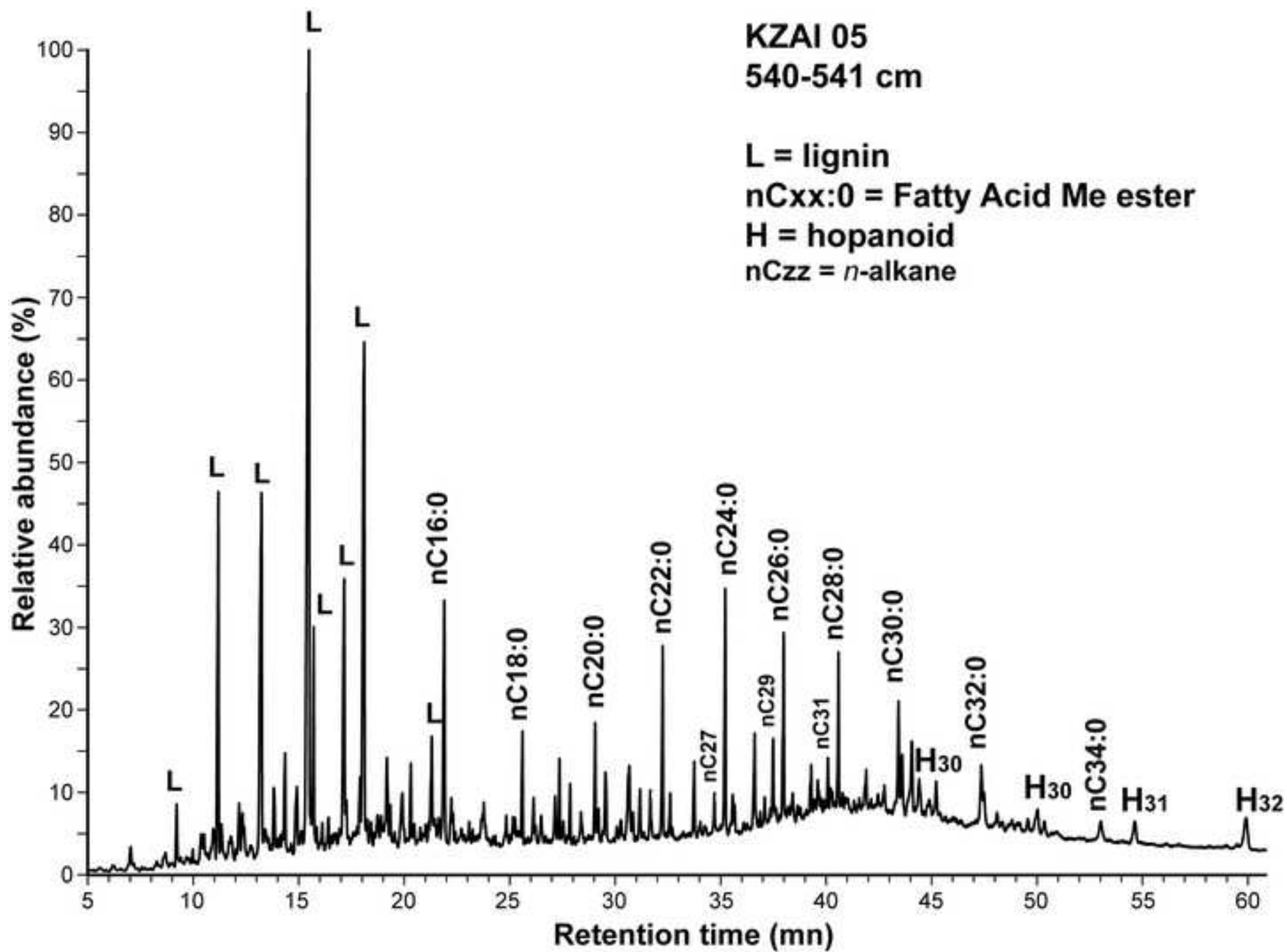


Figure 11
[Click here to download high resolution image](#)

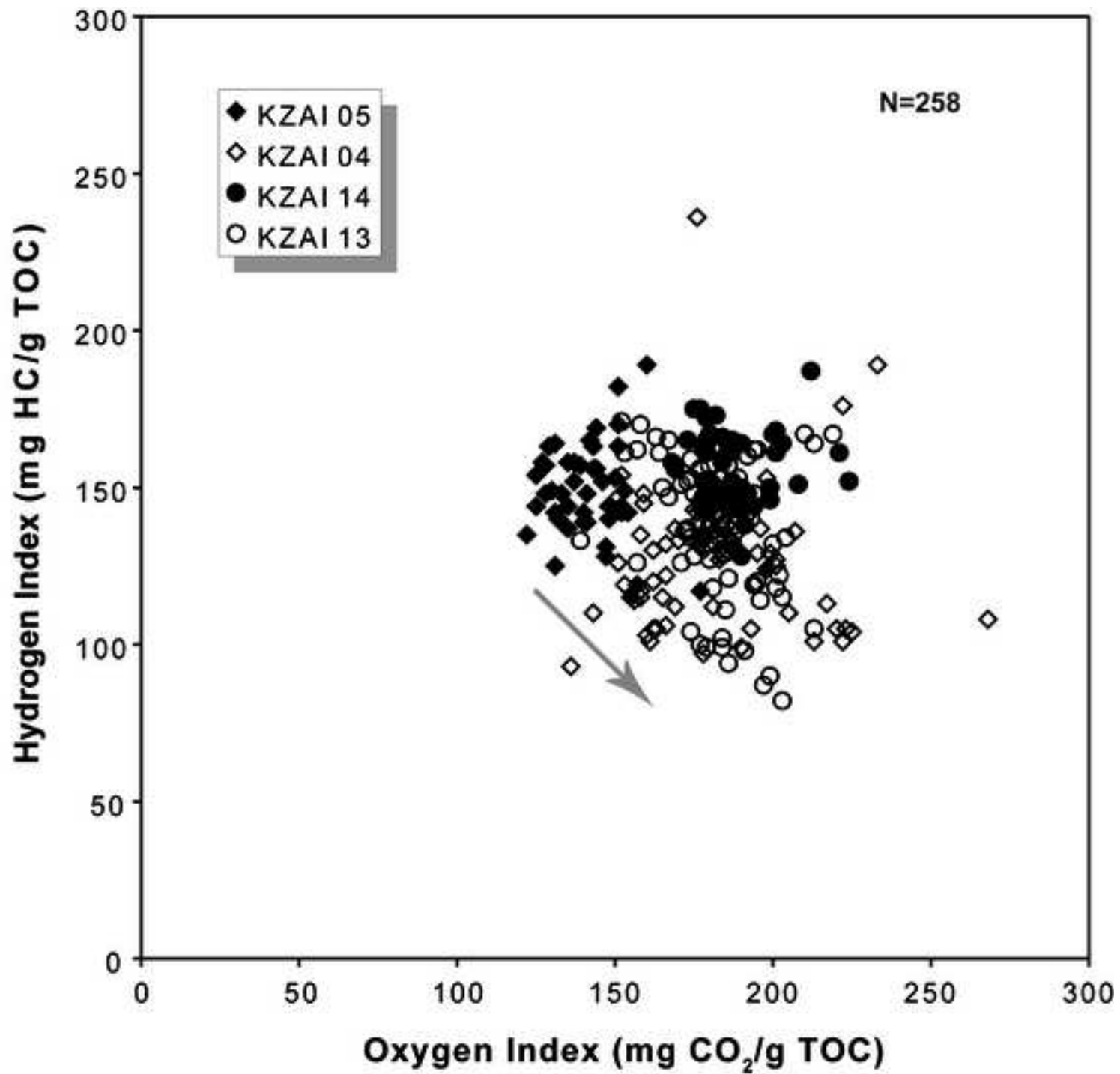


Table 1

| | Core | Lat. (°S) | Long. (°E) | Water depth (mbsl) | Situation | Penetration (mbsf) | Studied interval (m) | Number of samples | Mean spacing (m) |
|------------|-------------|------------------|-------------------|-------------------------------|------------------|-------------------------------|---------------------------------|------------------------------|-----------------------------|
| Upstream | KZAI 04 | 5° 48.04 | 8° 08.96 | 4047 | Levee | 16.87 | 10.0 | 83 | 0.12 |
| | KZAI 05 | 5° 44.50 | 8° 08.29 | 4012 | Crest of levee | 13.34 | 9.8 | 49 | 0.20 |
| | KZAI 06 | 5° 44.10 | 8° 08.23 | 4150 | Channel axis | 3.24 | 0.2 | 1 | - |
| Downstream | KZAI 13 | 5° 47.30 | 7° 13.89 | 4447 | Levee | 17.92 | 9.6 | 79 | 0.12 |
| | KZAI 14 | 5° 47.09 | 7° 13.98 | 4343 | Crest of levee | 17.3 | 10.0 | 100 | 0.10 |
| | KZAI 15 | 5° 46.62 | 7° 14.19 | 4433 | Channel axis | 1.93 | 0.6 | 4 | 0.15 |

Table 2

| | Core | Situation | Number of samples analysed | CaCO ₃ (%) | | TOC (%) | | HI (mg HC/g TOC) | | Number of samples analysed | C/N | | | δ ¹³ C (‰) | | | δ ¹⁵ N (‰) | | | | | |
|------------|---------|----------------|----------------------------|-----------------------|-------------|---------|------|------------------|------|----------------------------|------------|------|-----|-----------------------|--------------|------|-----------------------|---------------|--------|------|-------------|------|
| | | | | Min | Mean | Max | Min | Mean | Max | | Min | Mean | Max | Min | Mean | Max | Min | Mean | Max | | | |
| Upstream | KZAI 04 | Levee | 83 | 1.5 | 2.7 | 6.0 | 1.4 | 3.0 | 5.6 | 93 | 134 | 200 | 17 | 10.7 | 12.9 | 15.5 | -27.12 | -26.37 | -23.85 | 5.12 | 5.44 | 6.09 |
| | KZAI 05 | Crest of levee | 49 | 2.0 | 2.6 | 3.3 | 2.4 | 3.1 | 3.7 | 115 | 148 | 189 | 16 | 12.6 | 13.16 | 13.7 | -26.96 | -26.61 | -26.3 | 5.23 | 5.61 | 6.31 |
| Downstream | KZAI 13 | Levee | 79 | 0.8 | 2.6 | 3.3 | 0.1 | 2.97 | 4.04 | 82 | 137 | 171 | 16 | 11.8 | 13.09 | 15.7 | -26.17 | -25.94 | -25.46 | 4.98 | 5.47 | 5.98 |
| | KZAI 14 | Crest of levee | 100 | 1.33 | 2.5 | 3.25 | 0.85 | 3.08 | 3.9 | 128 | 163 | 236 | | | | | | | | | | |
| | KZAI 15 | Channel | 4 | 0.7 | 1.88 | 3.18 | 0.0 | 1.48 | 3.63 | 118 | 145 | 182 | | | | | | | | | | |

Table 3

| Core | Proxy | | | | |
|----------------|------------|-----------|-----------|------------------------------|------------------------------|
| | Mean HI | Max HI | N/C | $\delta^{13}\text{C}$ (‰) | $\delta^{15}\text{N}$ (‰) |
| KZAI 04 | 89 | 67 | 84 | 94 | 45 |
| KZAI 05 | 84 | 70 | 86 | 98 | 42 |
| KZAI 13 | 88 | 76 | 86 | 87 | 44 |
| KZAI 14 | 79 | 55 | | | |
| KZAI 15 | 85 | 73 | | | |
| Average | 85 | 67 | 85 | 93 | 44 |

Table 4

| Core | Depth (cm) | TOC (%) | S/V | (Vac+Sac)/ Ltot | (Vac+Sac)/ (Vald+Sald) | Ltot* | (nC16+nC18)FAMES* | C20+evenFAMES* |
|---------|------------|---------|------|--------------------|---------------------------|-------|-------------------|----------------|
| KZAI 04 | 1-2 | 1.54 | 0.30 | 0.65 | 2.56 | 32.2 | 8.9 | 19.5 |
| KZAI 04 | 297-298 | 2.60 | 0.33 | 0.60 | 1.74 | 36.2 | 5.4 | 5.7 |
| KZAI 05 | 2-3 | 2.40 | 0.45 | 0.62 | 2.02 | 40.1 | 8.2 | 16.5 |
| KZAI 05 | 540-541 | 3.28 | 0.59 | 0.56 | 1.83 | 45.0 | 7.6 | 26.4 |
| KZAI 05 | 960-961 | 3.45 | 0.33 | 0.62 | 2.05 | 33.9 | 7.2 | 12.5 |
| KZAI 13 | 540-541 | 3.20 | 0.61 | 0.59 | 2.37 | 46.3 | 7.4 | 18.7 |
| KZAI 13 | 926-927 | 2.42 | 0.57 | 0.55 | 1.75 | 48.2 | 3.8 | 13.7 |
| KZAI 13 | 928-929 | 2.42 | 0.56 | 0.55 | 1.81 | 48.4 | 5.4 | 15.8 |
| KZAI 15 | 4-5 | 1.59 | 0.36 | 0.61 | 1.98 | 34.4 | 7.5 | 13.0 |